

## On the Use of Ion-Selective Electrodes for Monitoring Oscillating Reactions. 2. Potential Response of Bromide- and Iodide-Selective Electrodes in Slow Corrosive Processes. Disproportionation of Bromous and Iodous Acids. A Lotka-Volterra Model for the Halate Driven Oscillators

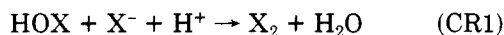
Z. Noszticzius,<sup>1</sup> E. Noszticzius,<sup>2</sup> and Z. A. Schelly\*

Department of Chemistry, The University of Texas at Arlington, Arlington, Texas 76019-0065 (Received: September 10, 1982; In Final Form: September 28, 1982)

The potential response of silver halide membrane electrodes to the corrosive bromous, bromic, iodous, and iodic acids is investigated in sulfuric acid solutions ( $[\text{H}_2\text{SO}_4] = 0.15$  and  $1.5$  M), typical media for several well-known oscillating reactions. The syntheses of the materials (bromide-free  $\text{NaBrO}_2$  and  $\text{HIO}_2$ ) needed for the experiments are described. The potentials recorded as a function of time were used for the determination or estimation of several rate constants at  $24 \pm 1$  °C: the disproportionation rate constant of  $\text{HBrO}_2$  is  $k_{B1} = (1.4 \pm 0.2) \times 10^3 \text{ M}^{-1} \text{ s}^{-1}$  (in  $0.15$  M  $\text{H}_2\text{SO}_4$ ) and  $(3.8 \pm 1.0) \times 10^3 \text{ M}^{-1} \text{ s}^{-1}$  (in  $1.5$  M  $\text{H}_2\text{SO}_4$ ); the corresponding value for  $\text{HIO}_2$  is  $k_{I1} < 5.4 \text{ M}^{-1} \text{ s}^{-1}$  (in  $0.05$ – $0.15$  M  $\text{H}_2\text{SO}_4$ ); the disproportionation of  $\text{HIO}_2$  is autocatalytic, the rate-determining step is a reaction of  $\text{HIO}_2$  with  $\text{H}_2\text{OI}^+$ , the rate constant of which is  $k_{I5} = 130 \pm 5 \text{ M}^{-1} \text{ s}^{-1}$  (in  $0.15$  M  $\text{H}_2\text{SO}_4$ ); the rate constants of the reactions of  $\text{HBrO}_2$  with  $\text{Br}^-$  and  $\text{H}^+$ , and  $\text{HIO}_2$  with  $\text{I}^-$  and  $\text{H}^+$  are  $10^6 < k_{B2} < 4 \times 10^6 \text{ M}^{-2} \text{ s}^{-1}$  (in  $1.5$  M  $\text{H}_2\text{SO}_4$ ) and  $10^6 < k_{I2} < 4 \times 10^7 \text{ M}^{-2} \text{ s}^{-1}$  (in  $0.15$  M  $\text{H}_2\text{SO}_4$ ), respectively. The corrosive reactions of the halous and halic acids with halide ions are much slower than those of hypohalous acids, which fact required the development of the theory for slow corrosive reactions. Criteria for the definitions of "slow" and "fast" corrosive reactions are given. The possibility of a second autocatalytic process in the halate driven oscillating reactions is demonstrated. On the basis of these results, a generalized Lotka-Volterra scheme is proposed for the BZ, BL, and BR oscillators.

### Introduction

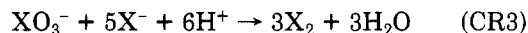
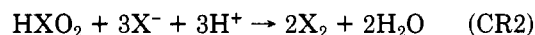
The present paper is the second communication in a series devoted to studying the potential response of ion-selective electrodes to corrosive species in oscillating chemical systems. The ultimate goal of our work is to provide a consistent interpretation of the potential changes displayed by bromide- and iodide-selective electrodes in the course of chemical oscillations, in terms of concentration changes of the several different intermediates involved. As a first step toward that goal, in a previous paper<sup>3</sup> we have shown that halide-ion-sensitive electrodes, besides halide ions, also respond to hypohalous acids. Furthermore, we have demonstrated that in the latter case the electrode response can be best explained by the corrosion potential theory (CPT). The corrosion reaction (CR) in question was the rapid removal of halide ions from the surface of silver-halide-based ion-selective electrodes by hypohalous acids according to the following equation



where  $\text{X} = \text{Cl}, \text{Br},$  or  $\text{I}$ .

The hypohalous acids are well-established corrosive intermediates of chemical oscillators (the Bray-Liebhaftsky (BL),<sup>4</sup> the Belousov-Zhabotinsky (BZ),<sup>5</sup> the Briggs-Rauscher (BR)<sup>6</sup> reactions and their modifications<sup>7,8</sup>) which have routinely been monitored with ion-selective electrodes; however, they are certainly not the only ones. In

strongly acidic media typical for oscillating reactions, halous ( $\text{HXO}_2$ ) and halic ( $\text{H}^+ + \text{XO}_3^-$ ) acids are also capable for analogous corrosive reactions in the following overall processes:



In this paper we present the results of our investigations on the potential responses with halous and halic acids of bromine and iodine in the solution. The corrosive reactions (CR2) and (CR3), however, are much slower than (CR1), requiring a modified mathematical treatment in the application of the CPT, and the establishment of criteria for the definitions of "slow" and "fast" corrosive reactions. A discussion of these problems is presented in the Theoretical Section.

Besides the extension of the CPT to relatively slow corrosive processes, we were able to synthesize bromous and iodous acids and measure the rates of their disproportionation in strongly acidic media.

We also investigated the reactions of the two halous acids with halogen and halide, to show the possibility of a second autocatalytic process in halate-driven oscillating reactions. Based on the results, we propose a generalized Lotka-Volterra scheme for the BZ, BL, and BR oscillators.

### Experimental Section

**Materials and Methods of Analysis.**  $\text{Ba}(\text{BrO}_2)_2$ . The synthesis of bromite salts and solutions is the subject of several patents.<sup>9-11</sup> Nevertheless, the details of the preparation are scanty, and a recent paper on the subject

(1) R. A. Welch Postdoctoral Fellow. On leave of absence from the Technical University of Budapest.

(2) R. A. Welch Predoctoral Fellow. On leave of absence from the Technical University of Budapest.

(3) Noszticzius, Z.; Noszticzius, E.; Schelly, Z. A. *J. Am. Chem. Soc.* 1982, 104, 6194-9.

(4) Bray, W. C.; Liebhaftsky, H. A. *J. Am. Chem. Soc.* 1931, 53, 38-48.

(5) Zhabotinsky, A. M. *Dokl. Akad. Nauk. USSR* 1967, 157, 392-400.

(6) Briggs, T. S.; Rauscher, W. C. *J. Chem. Ed.* 1973, 50, 469.

(7) Noyes, R. M. *J. Am. Chem. Soc.* 1980, 102, 4644-9.

(8) Cooke, D. O. *Int. J. Chem. Kinet.* 1980, 12, 683-98.

(9) Kircher, R.; Periat, R. German Patent 1 07 069, Feb 25, 1960.

(10) Meybeck, J.; Kircher, R.; Leclerc, J. U.S. Patent 3 085 854, April 16, 1963.

(11) Kricher, R.; Periat, R. U.S. Patent 3 095 267, June 25, 1963.

has reported that the direct synthesis of pure barium bromite was unsuccessful.<sup>12</sup> Our method is a modification of a procedure given by Kircher and Periat<sup>11</sup> for the preparation of crystalline barium bromite.

$\text{Ba}(\text{OH})_2 \cdot 8\text{H}_2\text{O}$  (100 g) was dissolved in 100 cm<sup>3</sup> of boiling distilled water. The undissolved  $\text{BaCO}_3$  was removed by filtration. The clear hot solution was cooled to 5–10 °C and the barium hydroxide crystals formed were collected by a subsequent filtration. The wet and easily soluble barium hydroxide (80 g) was cooled to 0 to –5 °C and a dropwise addition of bromine was started. The resulting slurry was stirred with a glass rod. When a liquid phase appeared, the mixture was cooled further to –5 to –10 °C. As the addition of bromine was continued, all barium hydroxide dissolved gradually, and later on a new solid phase (the dark yellow  $\text{Ba}(\text{BrO})_2$ ) appeared. After adding 8–9 cm<sup>3</sup> of liquid bromine, a pH-sensing glass electrode and a magnetic stirrer were inserted into the system. The bromine addition was stopped when the pH dropped to 11. (The total volume of the consumed bromine was about 10 cm<sup>3</sup>.) At this point the temperature was raised to –3 to –1 °C, and the stirring was continued for 2 h while maintaining the same temperature. During that period the pH was monitored and controlled between 10.7 and 11.3 by the addition of small amounts of  $\text{Br}_2$  (1–2 drops) or the freshly crystallized  $\text{Ba}(\text{OH})_2 \cdot 8\text{H}_2\text{O}$  (0.1–0.2 g), as needed. (The stirring and the continuous pH control are the crucial points of the preparation. The stirring is needed because most of the  $\text{Ba}(\text{BrO})_2$  starting material is in the solid phase at the beginning of the reaction but the disproportionation takes place in the liquid phase.) After 2 h, the reaction was stopped by stirring the mixture with 6 g of the wet barium hydroxide crystals for 5 min. A pale yellow solid formed and was collected by filtration. The wet product (~40 g) contained about 10 g of  $\text{Ba}(\text{BrO})_2 \cdot 2\text{H}_2\text{O}$ , less than 0.4 g of  $\text{Ba}(\text{BrO})_2$ , and considerable amounts of  $\text{BaBr}_2$ ,  $\text{Ba}(\text{BrO}_3)_2$ , and  $\text{Ba}(\text{OH})_2$ . The precipitate mixture was extracted with 150 cm<sup>3</sup> of distilled water at room temperature. The filtrate was concentrated to 50 cm<sup>3</sup> at ~35 °C by evaporation in vacuo. The barium bromite crystallizes on the glass surfaces, and it can be detached by cooling the evaporating flask to ~0 °C, then warming quickly with a hot water bath. About 8 g of wet barium bromite (canary yellow) was collected after filtration. This product was used without drying or further purification to prepare a stock solution of bromite in 0.1 M NaOH. (The trace amounts of  $\text{BaCO}_3$  precipitate formed during these manipulations did not disturb the subsequent experiments.) For the stock solution, typically 3 g of the wet barium bromite crystals was dissolved in 100 cm<sup>3</sup> of 0.1 M NaOH. Such a solution was practically free of hypobromite, and its bromate content was less than 5% of the bromite. The major disturbing contaminant was a trace amount of bromide.

*Bromide-free NaBrO<sub>2</sub> solution* was prepared from the bromite stock solution that contained two disturbing contaminants: barium and bromide ions. The  $\text{Ba}^{2+}$  could easily be removed as  $\text{BaSO}_4$  by an excess of sodium sulfate. (The sodium sulfate and the sodium hydroxide did not disturb our subsequent experiments in the concentration range applied.) The bromide ions were removed by freshly precipitated AgOH. As the solubility product of AgBr ( $K_s = 7.7 \times 10^{-13}$ , ref 13) is much smaller than that of AgOH ( $K_s = 1.58 \times 10^{-8}$ , ref 13) a precipitate-exchange reaction takes place leaving only  $[\text{Br}^-] < 10^{-5}$  M in the solution. At

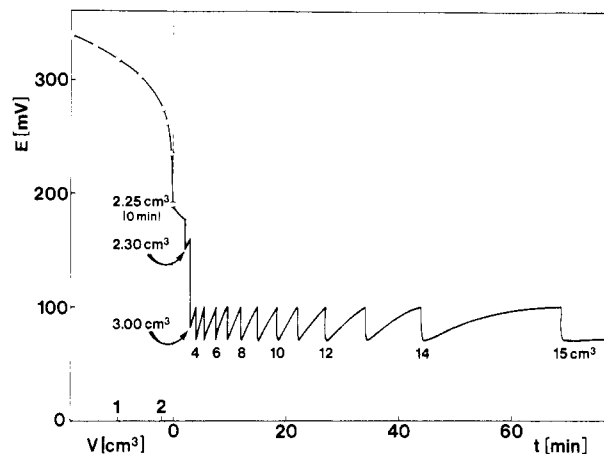


**Figure 1.** Potential  $E$  of the bromide-selective electrode vs. standard calomel electrode (SCE) during the titration with  $\text{Br}^-$  of an  $\text{HOBr}-\text{BrO}_3^-$  mixture formed in the disproportionation of bromous acid.  $\text{HBrO}_2$  was produced by injecting 2 cm<sup>3</sup> of bromide-free  $\text{NaBrO}_2$  solution ( $[\text{NaBrO}_2] = 2.25 \times 10^{-2}$  M determined by titration with arsenite) into 50 cm<sup>3</sup> of 1.5 M  $\text{H}_2\text{SO}_4$ . As  $\text{HOBr}$  reacts with bromide quickly, the first part of the curve depicts the potential as a function of the consumed titrant. The end point for  $\text{HOBr}$  was reached at 2.25 cm<sup>3</sup> of titrant added. Starting from that point, the potential was recorded as a function of time to follow the relatively slow reaction of bromate with bromide. The volume of the added titrant is indicated separately under the "saw tooth". Above 15 cm<sup>3</sup> of titrant added, no measurable change of potential could be detected, indicating that the solution had been over-titrated. Hence the bromate content of the solution required 11.75 cm<sup>3</sup> (14 cm<sup>3</sup> – 2.25 cm<sup>3</sup>) of  $10^{-2}$  M KBr titrant.

the same time, the silver contamination due to the solubility of AgOH was also negligible ( $[\text{Ag}^+] < 10^{-6}$  M).

In the actual purification, 5 cm<sup>3</sup> of 0.1 M  $\text{AgNO}_3$  and 1 cm<sup>3</sup> of 1 M NaOH were mixed in a 10-cm<sup>3</sup> volumetric flask. The brown AgOH precipitate was freed from its colloid fraction by decantation (4–5 times) with 0.1 M NaOH. Then 2 cm<sup>3</sup> of the bromite stock was added and shaken with the precipitate. A grayish color immediately appearing on the surface of AgOH indicated the presence of bromide. Subsequently, 2 cm<sup>3</sup> of 0.5 M  $\text{Na}_2\text{SO}_4$  were added to the mixture, and the flask was filled with 0.1 M NaOH. After filtration, the clear light-yellow barium- and bromide-free solution was analyzed and used in the experiments.

An independent source of  $\text{NaBrO}_2$  was a solution prepared at the Department of Physical Chemistry at the Philipps University in Marburg.<sup>14</sup> It was also freed of bromide by the above method before experiments. Our material and the Marburg sample yielded identical results.

*Analysis of the Bromite Solutions.* The stock solutions were not analyzed for bromide because that component could be removed quantitatively by AgOH. The hypobromite and bromite content of aliquot samples was determined separately in alkaline media by potentiometric titration with arsenite, using a platinum indicator electrode according to Andersen and Madsen.<sup>15</sup> (The bromite has to be titrated in the presence of osmium tetroxide catalyst. As even the catalyzed reaction is a bit slow, recording of the electrode potential during the titration is recommended.)

If the samples of the stock solution are introduced into acidic media (1.5 M  $\text{H}_2\text{SO}_4$ ) a fast disproportionation takes place (reaction B1). The hypobromous acid and the



(12) Sullivan, J. C.; Thompson, R. C. *Inorg. Chem.* 1979, 18, 2375–9.

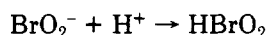
(13) "Handbook of Chemistry and Physics"; CRC Press: Cleveland, 1976–7; 57th ed, p B254.

(14) (a) Försterling, H. D.; Lamberz, H. J.; Schreiber, H. Z. *Naturforsch.* A 1980, 35, 1354–60. (b) Lamberz, H. J. Thesis, to be published.

(15) Andersen, T.; Madsen, H. E. L. *Anal. Chem.* 1965, 37, 49–51.

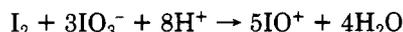
bromate produced this way could be determined separately by potentiometric titration with bromide in the presence of a bromide-selective indicator electrode (Figure 1). (The method is analogous to the titration of hypiodous acid and iodate with iodide.<sup>3</sup>) This second method of analysis provided independent data for checking the results of the arsenite titration, and an estimate for the bromate content according to the following considerations. The hypobromous acid content measured after the disproportionation was compared to a theoretical value calculated from the bromite and hypobromite (if there was any) content of the original basic samples. The measured and calculated data agreed within the experimental error of 2%. The original bromate content of a sample was estimated as the difference of the bromate concentration determined in the acidified sample and the bromate formed by the disproportionation of bromite.

**Instantaneous Production of  $\text{HBrO}_2$ .** First, 1 cm<sup>3</sup> of bromide-free  $\text{NaBrO}_2$  solution was diluted to 10 cm<sup>3</sup> with 0.1 M NaOH. Then 0.51 cm<sup>3</sup> of it was injected into 49.5 cm<sup>3</sup> of a vigorously stirred acidic solution ( $[\text{H}_2\text{SO}_4] = 1.5$  or 0.15 M), where the bromite reacts to form bromous acid<sup>14</sup>



The response of a bromide-selective electrode was recorded as a function of time (Figure 2, a and b).

**Preparation of Iodine(III) Solutions.** For the production of  $\text{HIO}_2$ , first we had to prepare iodine(III). It was discovered by Masson and Argument<sup>16</sup> that when mixing iodine and iodine pentoxide in concentrated sulfuric acid a liquid with a very pale yellow tint is formed. Its analysis corresponds to the sulfate of an oxide  $\text{I}_2\text{O}_3$  as the solute, and it was formulated as iodosyl sulfate  $(\text{IO})_2\text{SO}_4$ . According to Dasent and Waddington<sup>17</sup> it is rather probable that iodosyl sulfate has a polymeric structure in the solid state. In concentrated sulfuric acid solutions, however, much evidence is in favor of the formulation as  $\text{IO}^+$  for this I(III) species.<sup>18</sup> We prepared solutions of iodine(III) by dissolving iodine and potassium iodate in 96%  $\text{H}_2\text{SO}_4$ . The overall chemical reaction can be described as



Usually an excess of iodate was used to suppress the emergence of I(I). Actually in sulfuric acid media an equilibrium mixture of I(I), I(III), and I(V) exists and their relative amounts can be controlled by the initial  $[\text{I}_2]/[\text{IO}_3^-]$  ratio. To study the effect of the ratio, we prepared and tested three different solutions.

(i) Samples of 127 mg of  $\text{I}_2$  and 107 mg of  $\text{KIO}_3$  ( $[\text{IO}_3^-]/[\text{I}_2] = 1$ ) were dissolved in 25 cm<sup>3</sup> of 96%  $\text{H}_2\text{SO}_4$ . After 24 h, 1 cm<sup>3</sup> of the dark brown solution was diluted to 10 cm<sup>3</sup> with 96%  $\text{H}_2\text{SO}_4$ . The resulting solution (S1) contained a large amount of I(I).

(ii) Samples of 127 mg of  $\text{I}_2$  and 428 mg of  $\text{KIO}_3$  ( $[\text{IO}_3^-]/[\text{I}_2] = 4$ ) were dissolved in 25 cm<sup>3</sup> of 96%  $\text{H}_2\text{SO}_4$ . After 24 h, 1 cm<sup>3</sup> of the light yellow solution was diluted tenfold to result in solution S2.

(iii) Samples of 63.2 mg of  $\text{I}_2$  and 428 mg of  $\text{KIO}_3$  ( $[\text{IO}_3^-]/[\text{I}_2] = 8$ ) were dissolved in 25 cm<sup>3</sup> of 96%  $\text{H}_2\text{SO}_4$ . After 24 h, 2 cm<sup>3</sup> of the slightly yellowish solution was diluted to 10 cm<sup>3</sup> with 96%  $\text{H}_2\text{SO}_4$ , resulting in solution S3.

Solutions S2 and S3 contained mainly I(III) (and naturally also I(V)) and only a small amount of I(I).

**Instantaneous Production of  $\text{HIO}_2$ .** A 0.12-cm<sup>3</sup> sample of solution S1, S2, or S3 was injected into a well-stirred aqueous sulfuric acid solution (volume = 50 cm<sup>3</sup>,  $[\text{H}_2\text{SO}_4] = 0.15$  M, after the injection, except for the experiments in Figure 3d where the effect of  $[\text{H}_2\text{SO}_4]$  was examined). As is usually done, we presumed that in the dilute aqueous solution the iodosyl ion decomposes quickly, and that iodine(III) is present in the form of iodosous acid



The subsequent disproportionation of iodosous acid



was followed by recording the potential of an iodide-selective electrode as a function of time (Figure 3a,b).

**Stock Solutions of  $\text{Br}_2$ .** To avoid bromine losses due to evaporation from the concentrated stock, we prepared this by adding elementary bromine to 0.1–0.3 M NaOH. This way bromine was stored actually in the form of bromide and hypobromite and the elementary bromine was formed only when a small volume of the alkaline stock was injected into the 1.5 M  $\text{H}_2\text{SO}_4$  solution. (Changes in the sulfuric acid concentration due to dilution were below 1%, and the  $\text{Na}_2\text{SO}_4$  produced did not disturb our experiments.) So that disproportionation of the alkaline hypobromite was minimized, stock solutions were prepared freshly, and the  $[\text{NaOBr}]$  never exceeded 0.02 M (cf. Chapin<sup>19</sup>).

**Stock solutions of  $\text{I}_2$**  were prepared by dissolving a weighed amount of iodine in methanol. The stock was further diluted with water before use. The methanol content was always below 1% in the final solutions, which had no measurable effect on the experiments.

**Silver-free  $\text{HOBr}$**  was prepared as described previously.<sup>3</sup>

All other chemicals were of reagent grade and used without further purification.

**The experimental setup** and the preparation of the electrodes were described previously.<sup>3</sup> The same current bridge chain containing 10 M  $\text{NH}_4\text{NO}_3$  solution was used with a saturated KCl calomel reference electrode. All the reported  $E$  values (sometimes simply termed as "electrode potentials") are electromotive forces measured in galvanic cells, consisting of the silver halide membrane electrode, salt bridge chain, and reference electrode. The experiments were carried out at  $24 \pm 1$  °C.

## Results and Discussion

**I. Disproportionation of Bromous Acid.** The potential response of the bromide-selective electrode as a function of time, after the instantaneous production of  $\text{HBrO}_2$  in 0.15 and 1.5 M  $\text{H}_2\text{SO}_4$ , is shown in Figure 2, a and b. The remarkable feature of the curves is that the potential change is significantly slower compared to that caused by pure  $\text{HOBr}$  (also depicted in the same figures). Thus, it is reasonable to assume that a chemical reaction takes place during the measurement, on a time scale much exceeding the less than 1 s required for the complete mixing of  $\text{NaBrO}_2$  with the  $\text{H}_2\text{SO}_4$  solution. We are going to show that this reaction is the disproportionation (B1) of  $\text{HBrO}_2$ , and that it is much slower than previously assumed in the literature.<sup>14–20</sup> Since the contribution of the bromous acid to the corrosion potential is negligible in the concentration range used (see the section on slow corrosive processes), we can also show that the electrode potential, after the first

(16) Masson, I.; Argument, C. *J. Chem. Soc.* 1938, 1702–8.

(17) (a) Dasent, W. E.; Waddington, T. C. *J. Chem. Soc.* 1960, 3350–6.

(b) *J. Inorg. Nucl. Chem.* 1963, 25, 132–3.

(18) Masson, I.; Hanby, W. E. *J. Chem. Soc.* 1938, 1699–701.

(19) Chapin, R. M. *J. Am. Chem. Soc.* 1934, 56, 2211–5.

(20) Field, R. J.; Körös, E.; Noyes, R. M. *J. Am. Chem. Soc.* 1972, 94, 8649–64.

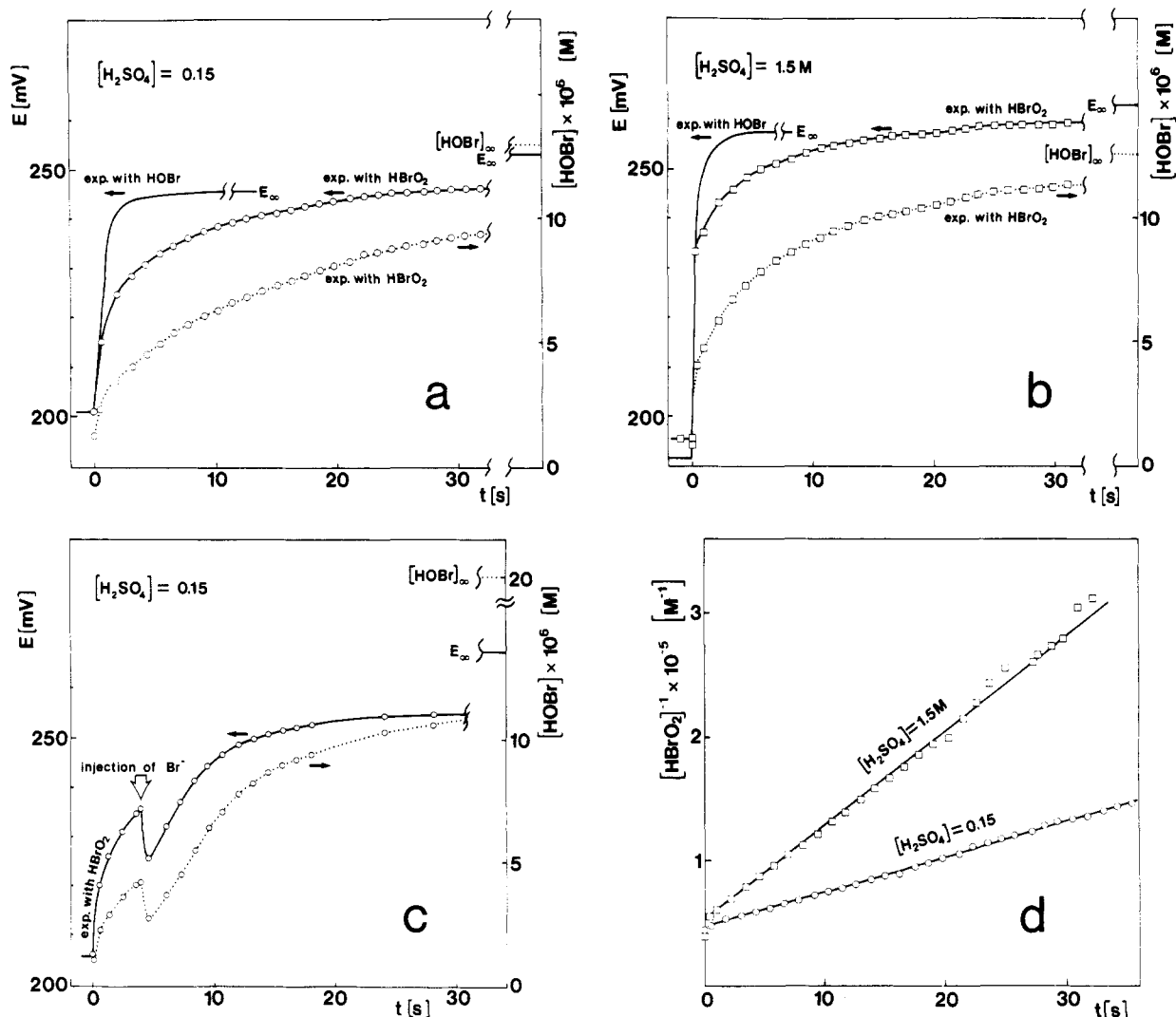


**Figure 2.** (a) Potential  $E$  of the bromide-selective electrode as a function of time  $t$  after the addition of the following solutions to  $49.5 \text{ cm}^3$  of  $0.15 \text{ M H}_2\text{SO}_4$  in each case:  $0.51 \text{ cm}^3$  of  $10^{-3} \text{ M HOBr}$  (curve "exp. with HOBr"), and  $0.51 \text{ cm}^3$  of  $2.25 \times 10^{-3} \text{ M NaBrO}_2$  (curve "exp. with  $\text{HBrO}_2$ "). Dotted curve (right scale):  $[\text{HOBr}]$  as a function of time, calculated from the potentials given by the solid  $\text{HBrO}_2$  curve. The points at which the calculations were carried out are marked by (O). (b) Same as (a) except  $[\text{H}_2\text{SO}_4] = 1.5 \text{ M}$ . Points of the calculations are marked by ( $\square$ ). (c) Electrode potential  $E$  (solid line) and the corresponding calculated  $[\text{HOBr}]$  (dotted line, right scale) as a function of time  $t$  after the addition of  $0.51 \text{ cm}^3$  of  $2.25 \text{ M NaBrO}_2$  (at  $t = 0$ ) and  $0.65 \text{ cm}^3$  of  $10^{-3} \text{ M KBr}$  (at  $t = 4 \text{ s}$ ) to  $49.5 \text{ cm}^3$  of  $0.15 \text{ M H}_2\text{SO}_4$ . Points of calculation are marked by (O). (d) Reciprocal  $[\text{HBrO}_2]^{-1}$  as a function of time  $t$ . Calculated from the data of the dotted lines in Figure 2, a and b.

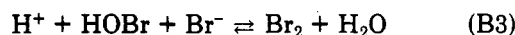
2–3 s, is controlled exclusively by the concentration of HOBr, slowly produced from  $\text{HBrO}_2$ .

One can test the hypothesis about the slowness of the disproportionation by checking if  $\text{HBrO}_2$  is still present, say 4 s after its formation. To do this, first we determined the total HOBr formed in a run with complete disproportionation of  $\text{HBrO}_2$ , by potentiometric titration with  $\text{Br}^-$ . In a subsequent experiment, we injected the predetermined equivalent quantity of  $\text{Br}^-$  (that would be needed in case of completed disproportionation) into the  $\text{HOBr}_2$  solution, after 4 s of its formation (Figure 2c). As the potential response indicates, after the rapid removal by  $\text{Br}^-$  of HOBr formed during the first 4 s of disproportionation, additional HOBr was formed in the net process

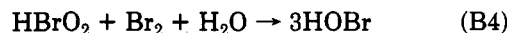


resulting in a higher amount of HOBr present at the end of the reaction than would have been without adding the bromide! This result indicates that reaction B1 is slow enough for having unreacted  $\text{HBrO}_2$  present even after 4 s of disproportionation. Clearly, in the presence of  $\text{Br}^-$ , both (B1) and (B2) contribute to the formation of HOBr and thus to the observed potential. Naturally if  $\text{Br}^-$  is added, the actual pathway includes the formation of some

elementary bromine as well, since HOBr reacts with  $\text{Br}^-$  much faster than  $\text{HBrO}_2$ , in reaction B3:



As another possibility, the bromous acid may also react directly with  $\text{Br}_2$  formed as follows:



Nevertheless, (B2) is essentially the sum of the reactions B3 and B4.

To determine the rate constant  $k_{\text{B1}}$  of the disproportionation reaction B1, one has to obtain the  $[\text{HBrO}_2]$  values as a function of time  $t$ . If the stoichiometry of the disproportionation is used,  $[\text{HBrO}_2]_t$  can be calculated from

$$[\text{HBrO}_2]_t = 2([\text{HOBr}]_\infty - [\text{HOBr}]_t) \quad (1)$$

Since the measured potentials  $E$  are solely determined by HOBr,  $[\text{HOBr}]_t$  can be obtained from  $E_t$  if a reference point for the relationship between the two is first established. We chose  $E_\infty$  as a reference point, because at  $t \rightarrow \infty$  the disproportionation of  $\text{HBrO}_2$  is complete and  $[\text{HOBr}]_\infty$  can be accurately determined by potentiometric titration. The silver ion concentration at the electrode surface is established by the presence of corrosive HOBr.

TABLE I: HOBr Production from HBrO<sub>2</sub> in Acidic Solutions Containing Br<sub>2</sub> and/or Br<sup>-</sup> ([H<sub>2</sub>SO<sub>4</sub>] = 0.15 M)

10 <sup>5</sup> [HBrO <sub>2</sub> ] <sub>0</sub> /M <sup>a</sup>				2.28					
10 <sup>5</sup> [Br <sub>2</sub> ] <sub>0</sub> /M <sup>b</sup>	0	0.4	0.82	2.1	4.3	8.6	22	0	
10 <sup>5</sup> [Br <sup>-</sup> ] <sub>0</sub> /M <sup>c</sup>	0	0.04	0.06	0.09	0.13	0.18	0.29	2.4	
10 <sup>5</sup> [HOBr] <sub>∞</sub> /M <sup>d</sup>	1.3	2	2.4	3.2	3.7	4.0	3.7	2.1	

<sup>a</sup> The initial bromous acid concentration [HBrO<sub>2</sub>]<sub>0</sub> was calculated from the amount of the NaBrO<sub>2</sub> injected into the acidic solution containing Br<sub>2</sub> and/or Br<sup>-</sup>. <sup>b</sup> The initial bromine concentration [Br<sub>2</sub>]<sub>0</sub> was computed from the amount of bromine introduced originally to the solution and its subsequent hydrolysis. <sup>c</sup> The initial bromide concentration [Br<sup>-</sup>]<sub>0</sub> was calculated from the hydrolysis equilibrium of bromine as no bromide was added to the solution directly except the last experiment where the solution contained only Br<sup>-</sup>. <sup>d</sup> [HOBr]<sub>∞</sub> was determined by titration with 10<sup>-3</sup> M KBr solution.

If [Ag<sup>+</sup>] is computed at the reference point based on a theoretical expression (2) we derived previously<sup>3</sup>

$$[\text{Ag}^+]_{\infty} = f([\text{HOBr}]_{\infty}) \quad (2)$$

and if ideal Nernstian response is assumed for the interfacial silver ions, their concentration at time *t* can be expressed as

$$[\text{Ag}^+]_t = [\text{Ag}^+]_{\infty} \times 10^{(E_t - E_{\infty})/59 \text{ mV}} \quad (3)$$

Finally, the hypobromous acid concentration in the bulk at time *t* (to be used in eq 1) can be computed from

$$[\text{HOBr}]_t = f^{-1}([\text{Ag}^+]_t) \quad (4)$$

Since the rate equation of (B1) should be<sup>14,21</sup>

$$d[\text{HBrO}_2]/dt = -2k_{\text{B1}}[\text{HBrO}_2]^2 \quad (5)$$

the slope (2*k*<sub>B1</sub>) of 1/[HBrO<sub>2</sub>] vs. time (Figure 2d) yields the rate constant. At the two sulfuric acid concentrations investigated, the results are

$$k_{\text{B1}} = (1.4 \pm 0.2) \times 10^3 \text{ M}^{-1} \text{ s}^{-1} \text{ in } 0.15 \text{ M H}_2\text{SO}_4$$

$$k_{\text{B1}} = (3.8 \pm 1.0) \times 10^3 \text{ M}^{-1} \text{ s}^{-1} \text{ in } 1.5 \text{ M H}_2\text{SO}_4$$

It is interesting to note that another possible mechanism for the disproportionation



followed by (B2) would result in (B1) as a net reaction. This autocatalytic mechanism can play an important role at higher pH values and HOBr concentrations.<sup>22</sup> The rather good second-order plots in Figure 2d indicate, however, that this pathway is negligible in our case.

*Possible Sources of Error.* The uncertainties in the numerical values reported for *k*<sub>B1</sub> are not standard deviations (they would have been smaller by one order of magnitude), but rather estimates based on considerations of some possible systematic error sources.

(i) *Error due to Slow Mixing.* The finite time required for mixing and for electrode response can affect only the first 2–3 s of the measurements. To minimize this error, samples were always injected within 0.3 s into the center of the vortices of vigorously stirred solutions.

(ii) *Errors due to Nonideal Electrode Behavior.* To a certain extent, the electrode potential depends on the “history” of the electrode. E.g., after performing some measurements in a medium containing bromine or hypobromous acid, the electrode potential can rise several millivolts in the subsequent experiment. Fortunately, this “memory effect” is pronounced only in the region of non-Nernstian response at the very beginning of a measurement. The reference point (*E*<sub>∞</sub>, [HOBr]<sub>∞</sub>) method described in the previous section was introduced to minimize errors due to such effects. Nevertheless, since the beginning of a single measurement represents a “history” for the

end of the same measurement, an uncertainty of ±1 mV is conceivable in the reference potentials *E*<sub>∞</sub>.

(iii) *Errors Caused by Organic Traces.* Organic traces present in distilled water react with HOBr (and HBrO<sub>2</sub>) to produce Br<sub>2</sub>. In turn, if HBrO<sub>2</sub> is present, it reacts with the elementary bromine to form HOBr (see later). The effects of organic traces becomes significant in very dilute solutions (10<sup>-5</sup> M or less) of HOBr and HBrO<sub>2</sub> even with the exclusive use of bidistilled water. Typically, as determined by potentiometric titration with KBr, in 1.5 M H<sub>2</sub>SO<sub>4</sub> solutions of 1 × 10<sup>-5</sup> M HOBr or HBrO<sub>2</sub> we found a ~20% loss or a ~10% excess, respectively, due to reactions with organic traces. During the measurement of the disproportionation, however, only that fraction of the organic trace which reacts at a rate comparable to that of the disproportionation causes an actual error. The effect of much faster or slower reactions can be neglected. (The hypobromous acid produced in faster reactions causes an “initial” [HOBr]<sub>0</sub> that drops out in the computation of [HBrO<sub>2</sub>]<sub>t</sub> as an additive constant according to eq 1. The effect of slower reactions cannot be observed on the time scale of the experiments.) Consequently, the 10–20% relative difference between the actual and expected HOBr concentrations represents the upper limit for the error caused by organic traces.

*Comparison of *k*<sub>B1</sub> with Previous Results.* The disproportionation of bromous acid plays an important role in the mechanism of the oscillatory Belousov–Zhabotinsky reaction. In fact, it is one of the five basic reactions forming the Oregonator model<sup>23</sup> which is a skeletonized version of the well-known FKN mechanism.<sup>20</sup> In strong acidic media prevailing in the BZ systems, however, no attempt was made previously to measure directly the rate of disproportionation. Thus, in the past decade most of the numerical simulations of the BZ reactions<sup>24,25</sup> used a theoretical estimate of *k*<sub>B1</sub> = 4 × 10<sup>7</sup> M<sup>-1</sup> s<sup>-1</sup> ([H<sub>2</sub>SO<sub>4</sub>] = 0.8 M) which is four orders of magnitude larger than our result. Sullivan and Thompson<sup>12</sup> showed experimentally that this value is too high, and also an extrapolation of data obtained by Massagli et al.<sup>22</sup> suggests a much smaller actual *k*<sub>B1</sub>. Our measurements support the later expectations.

*Observations on the Reaction of HBrO<sub>2</sub> with Br<sub>2</sub> and Br<sup>-</sup>. A Lotka–Volterra Model for the BZ Reaction.* We attempted to obtain information about the rates of reactions B2–B4 by injecting the NaBrO<sub>2</sub> solutions into acidic media already containing Br<sub>2</sub> and Br<sup>-</sup>. The conversion of bromide to bromine in reactions B2 and B3 is too fast to be followed by our method: within the time of mixing an excess of HOBr appeared both in 0.15 and 1.5 M H<sub>2</sub>SO<sub>4</sub>. On the basis of this observation, a lower limit for *k*<sub>B2</sub> (>10<sup>6</sup> M<sup>-2</sup> s<sup>-1</sup>) can be estimated. Afterward, in a slower reaction regime, more HOBr was produced by reactions B1 and B4. When the electrode potential reached a stationary value,

(21) Noyes, R. M.; Field, R. J.; Thompson, R. C. *J. Am. Chem. Soc.* **1971**, *93*, 7315–6.

(22) Massagli, A.; Indelli, A.; Pergola, F. *Inorg. Chim. Acta* **1970**, *4*, 593–6.

(23) Field, R. J.; Noyes, R. M. *J. Chem. Phys.* **1974**, *60*, 1877–84.

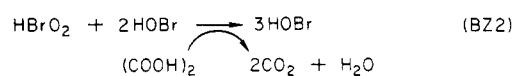
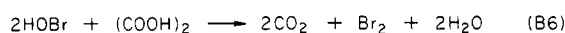
(24) Edelson, D.; Field, R. J.; Noyes, R. M. *Int. J. Chem. Kinet.* **1975**, *7*, 417–32.

(25) Edelson, D.; Noyes, R. M.; Field, R. J. *Int. J. Chem. Kinet.* **1979**, *9*, 155–64.

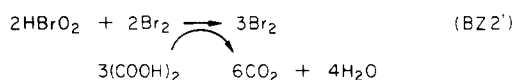
the total  $[\text{HOBr}]_{\infty}$  produced was determined by titration. The results of these preliminary experiments are summarized in Table I. The most interesting point of the data is that  $[\text{HOBr}]_{\infty}$  increases significantly with  $[\text{Br}_2]_0$ , indicating that reaction (B4) can compete with (B1) even at very low bromine concentrations. (The reason for  $[\text{HOBr}]_0$  going through a maximum in Table I is not known at the present time.)

From our preliminary data it is not clear whether the reaction between  $\text{Br}_2$  and  $\text{HBrO}_2$  is a result of the hydrolysis of  $\text{Br}_2$  followed by reaction B2, or also of a direct attack as in (B4). Anyway, (B4) may play an important role also in the BZ reactions, especially in those systems where elementary bromine seems to appear in rate-controlling steps.<sup>26,27</sup> The theoretical consequences of such a hypothesis will be analyzed in detail in a subsequent paper. For the time being, we only wish to make a few brief remarks.

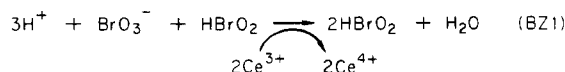
In BZ systems where some reducing organic material is present, the appearance of a second *autocatalytic process* may be of intrinsic importance. In the simplest case the organic substrate is oxalic acid.<sup>26</sup> Since oxalic acid reacts readily with  $\text{HOBr}$ ,<sup>28</sup> the following scheme can be constructed:



or by combining 2 × (B4) and 3 × (B6)



In a general case, of course, other organic substrates can play the role of oxalic acid. Therefore, either reaction BZ2 or BZ2' as a second autocatalytic process together with the well-established first one proposed by Noyes, Field, and Thompson<sup>21</sup>



can form a Lotka–Volterra<sup>29,30</sup> type “core”<sup>31</sup> for the BZ systems.

**II. Disproportionation of Iodous Acid.** The potential response of the iodide-selective electrode as a function of time after the instantaneous production of  $\text{HIO}_2$  from different solutions containing iodine(III) is shown in Figure 3a. There are several analogies between the behavior of  $\text{HBrO}_2$  and  $\text{HIO}_2$ , but important differences can be observed as well. (i) The potential change is much slower than in the case of bromous acid. We shall show that this is caused by the slow production of  $\text{H}_2\text{OI}^+$  through the disproportionation of  $\text{HIO}_2$ . (ii) During the first 20–30 min, the potential increases because  $\text{H}_2\text{OI}^+$  is more corrosive than  $\text{HIO}_2$  or acidic iodate (see later), thus the electrode potential is controlled solely by the  $[\text{H}_2\text{OI}^+]$ . (iii) There is a sudden jump in the electrode potential immediately

TABLE II: Titration Results for Iodous–Hypoiodous Acid Mixtures in Different Stages of the Disproportionation of  $\text{HIO}_2$ <sup>a</sup>

experiment <sup>b</sup>	A	B	C	D	E
$t/\text{min}^c$	~0.5	~5	~10	~20	~30
$V_t/\text{cm}^{3d}$	3.2	2.5	2.15	1.35	0.75
$\alpha/\%^e$	13	37	48	75	95

<sup>a</sup> Initial iodous acid concentration,  $[\text{HIO}_2]_0 = 2.4 \times 10^{-5} \text{ M}$ ,  $[\text{H}_2\text{SO}_4] = 0.15 \text{ M}$ . <sup>b</sup> Experiments A–E are depicted in Figure 3c. <sup>c</sup>  $t$  is the time of disproportionation  $\approx$  time elapsed until starting titration. <sup>d</sup>  $V_t$  is the volume of the required  $10^{-3} \text{ M}$  KI titrant. <sup>e</sup>  $\alpha$  is the degree of disproportionation,  $\alpha \equiv ([\text{HIO}_2]_0 - [\text{HIO}_2]_t) / ([\text{HIO}_2]_0) \times 100\%$ .  $[\text{HIO}_2]_t$  is the iodous acid concentration at the moment  $t$  (calculated disregarding any further decomposition of  $\text{H}_2\text{OI}^+$ ).

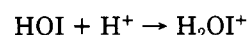
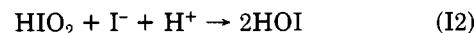
after the injection of the iodine(III) samples (preceding the aforesaid slow rise), where the height of the jump depends on the composition of the solution (S1, S2, or S3) added (Figure 3a). (iv) While the disproportionation of  $\text{HOBr}$  was negligible on the time scale of the experiment, it can easily be observed for  $\text{H}_2\text{OI}^+$ : its concentration (and thus the potential) go through a maximum (Figure 3, a and b). A practical problem associated with the disproportionation of  $\text{H}_2\text{OI}^+$  is that a different electrode-calibration procedure is needed, because here the presence of a significant level of  $\text{HIO}_2$  disturbs the volumetric determination of  $[\text{H}_2\text{OI}^+]_{\infty}$  by KI. (v) In contrast to bromous acid, the kinetics of the disproportionation of  $\text{HIO}_2$  is clearly not a simple second-order decomposition, but rather an autocatalytic production of  $\text{H}_2\text{OI}^+$  (see the sigmoid shape of the  $[\text{H}_2\text{OI}^+]$  curve in Figure 3b). (vi) Contrary to  $\text{HBrO}_2$ , the rate of disproportionation of  $\text{HIO}_2$  decreases with increasing sulfuric acid concentration in the range of  $0.05 \text{ M} < [\text{H}_2\text{SO}_4] < 0.15 \text{ M}$  (Figure 3d).

In the following, we shall discuss observations (i) to (vi) in detail, and propose a simple mechanism for the autocatalytic disproportionation of iodous acid.

(i) Since the process I1 was observed to be much slower than expected according to theoretical estimates,<sup>32–34</sup> it was necessary to show that the slow potential change is due to the slow production of  $\text{H}_2\text{OI}^+$ . As process I1 is considerably slower than (B1), one has sufficient latitude to perform titrations with KI at several different stages of the reaction (Table II and Figure 3c).

The later the titration is performed the smaller is the volume of titrant consumed. This can be understood by assuming that a disproportionation of the iodous acid takes place in (I1), where 2 mol of  $\text{HIO}_2$  produces only 1 mol of  $\text{H}_2\text{OI}^+$ . Since 1 mol of  $\text{HIO}_2$  consumes three times as much iodide as 1 mol of  $\text{H}_2\text{OI}^+$ , the volume of  $10^{-3} \text{ M}$  KI required decreases as a function of time at which the titration is performed (Table II).

In titrations performed at early stages of the disproportionation, the potential is first rising (!) when KI titrant is added, and at a rate faster than prior to addition. Again the presence of  $\text{HIO}_2$  explains the observation, if it is available in considerable amount and reacts with  $\text{I}^-$  to form additional  $\text{H}_2\text{OI}^+$  in (I2) and the subsequent protonation of HOI



and the potential rises as a consequence of the increasing  $\text{H}_2\text{OI}^+$  concentration. Since hypoiodous acid reacts much

(26) Noszticzius, Z.; Bodiss, J. *J. Am. Chem. Soc.* **1979**, *101*, 3177–82.

(27) Noszticzius, Z.; Bodiss, J. *Ber. Bunsenges. Phys. Chem.* **1980**, *84*, 366–9.

(28) Knoller, Y.; Perlmutter-Hayman, B. *J. Am. Chem. Soc.* **1955**, *77*, 3212.

(29) Lotka, A. J. *J. Am. Chem. Soc.* **1920**, *42*, 1595–9.

(30) Volterra, V. “Animal Ecology”, Chapman, R. W., Ed.; McGraw-Hill: New York, 1931, pp 409–48.

(31) Noszticzius, Z.; Farkas, H. “Modelling of Chemical Reaction Systems”, Ebert, K. H.; Deufhard, P.; Jager, W., Ed.; Springer: Berlin, 1981; pp 275–81.

(32) Edelson, D.; Noyes, R. M. *J. Phys. Chem.* **1979**, *83*, 212–20.

(33) Furrow, S. D.; Noyes, R. M. *J. Am. Chem. Soc.* **1982**, *104*, 38–42.

(34) DeKepper, P.; Epstein, I. R. *J. Am. Chem. Soc.* **1982**, *104*, 49–55.

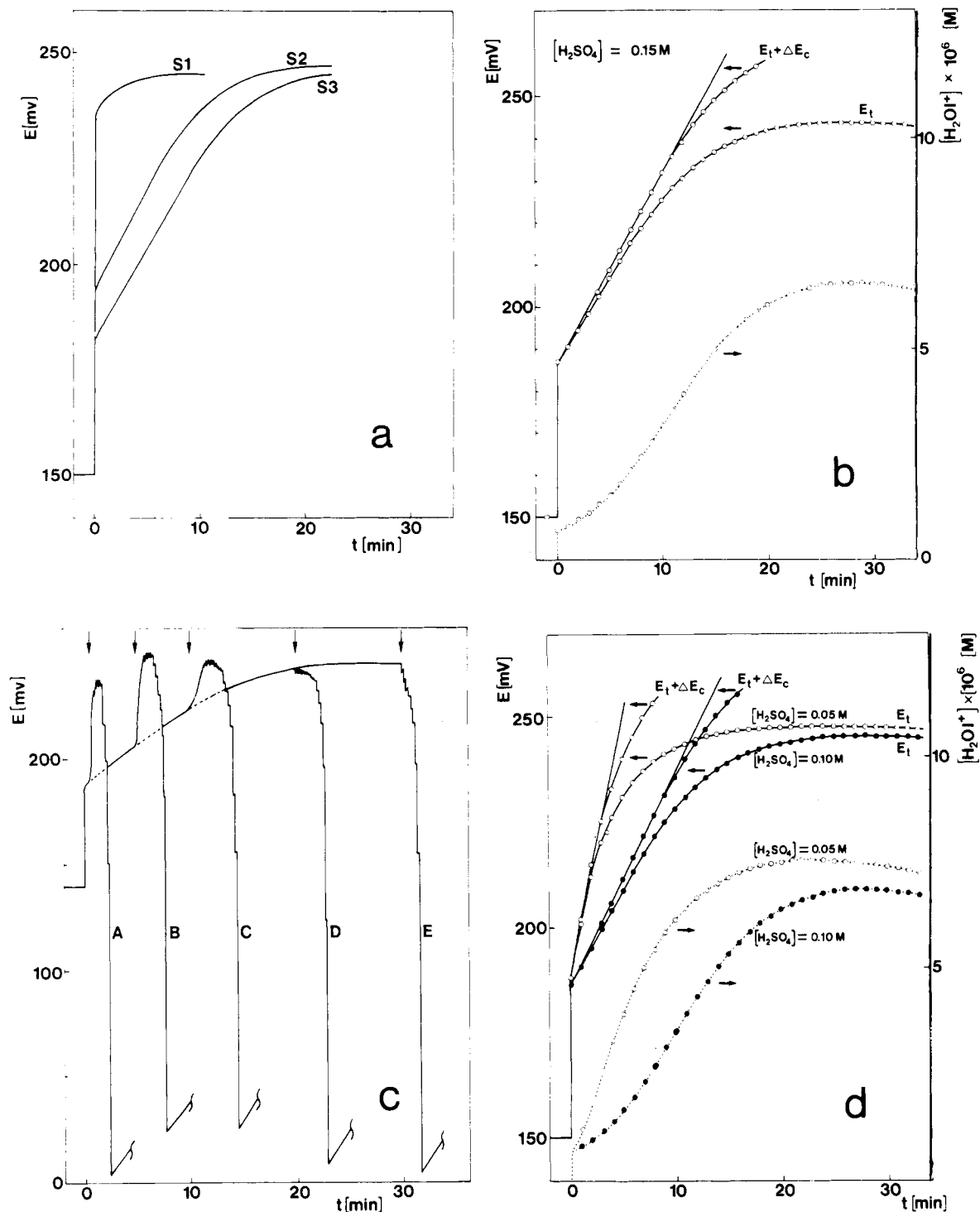
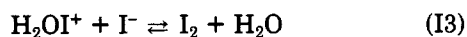


**Figure 3.** (a) Potential  $E$  of the iodide-selective electrode as a function of time  $t$  after the addition of the following solutions to  $36 \text{ cm}^3$  of  $0.15 \text{ M H}_2\text{SO}_4$  in each case:  $0.12 \text{ cm}^3$  of S1 (curve S1),  $0.12 \text{ cm}^3$  of S2 (curve S2), and  $0.12 \text{ cm}^3$  of S3 (curve S3). Also  $14 \text{ cm}^3$  of  $\text{H}_2\text{O}$  was added simultaneously in each experiment to maintain a sulfuric acid concentration of  $0.15 \text{ M}$ . (Preparation of solutions S1–S3 is described in the Experimental Section.) (b) Experimental conditions are the same as in Figure 3a, solution S3. The hypodous acid concentration  $[\text{H}_2\text{OI}^+]$  (dotted curve, right scale) and the corrected electrode potential  $E_t + \Delta E_c$  (solid curve,  $E_t + \Delta E_c$  left scale) was calculated from  $E_t$  values (solid curve,  $E_t$  left scale) according to the text. The points at which the calculations were carried out are marked by (O). (c) Experimental conditions are the same as in Figure 3b except titration was performed at different times in different experiments (A–E) shown in the figure. KI titrant ( $10^{-3} \text{ M}$ ) was added in  $0.5\text{-cm}^3$  (A),  $0.2\text{-cm}^3$  (B), and  $0.1\text{-cm}^3$  (C,D,E) portions except near the equivalence point where  $0.05\text{-cm}^3$  steps were used. See Table II for the results of the titrations. (d) The effect of the sulfuric acid concentration on the disproportionation of iodous acid. Applied sample:  $0.12 \text{ cm}^3$  of S3. Final volume is  $50 \text{ cm}^3$ . Final sulfuric acid concentration is  $0.1$  and  $0.05 \text{ M}$ , respectively. The notation of the variables is the same as in Figure 3b except points used for calculations are marked by full circles (●) in the case of  $0.1 \text{ M H}_2\text{SO}_4$  and by open circles (O) in the case of  $0.05 \text{ M H}_2\text{SO}_4$  media.

faster with iodide than iodous acid (see later), the actual pathway for process I2 includes the establishment of a quasi-preequilibrium



followed by (I2) or, perhaps, a direct reaction between iodine and iodous acid can also take place



Although, according to (I2) to (I4) both  $\text{H}_2\text{IO}^+$  and  $\text{HIO}_2$

can be titrated with HI, no separate determination of these acids can be carried out this way. Nevertheless, the presence of iodous acid can be detected qualitatively even where the potential reaches the stationary regime. Namely, when adding a small amount of KI titrant to the solution, first the potential drops suddenly because of (I3). But then, additional hypoiodous acid is produced from HIO<sub>2</sub> (in (I4), or (I2) coupled with the backward reaction of (I3)) and the potential rises again. All the titration curves in Figure 3c offer clear signs of the presence of iodous acid. (See the zigzag shaped noiselike portion of the curves, where each tiny peak corresponds to the addition of KI.)

Since also H<sub>2</sub>OI<sup>+</sup> disproportionates with a measurable rate leading to the buildup of an unknown concentration of I<sub>2</sub>, no exact evaluation of the results of the titration is possible. However, the extent of the disproportionation of HIO<sub>2</sub> can be estimated by disregarding the disproportionation of H<sub>2</sub>OI<sup>+</sup>. With such an approximation, based on the stoichiometry of (I1), the following material balance can be written

$$[\text{HIO}_2]_0 = [\text{HIO}_2]_t + 2[\text{H}_2\text{OI}^+]_t \quad (6)$$

where the subscripts refer to values of time. The volume of titrant required at times 0 and *t* are given by

$$V_0 = C \times 3[\text{HIO}_2]_0 \quad (7)$$

$$V_t = C(3[\text{HIO}_2]_0 + [\text{H}_2\text{OI}^+]) \quad (8)$$

where *C* is a proportionality factor. The degree of disproportionation  $\alpha$  in Table II was calculated by the use of eq 9 which can be derived from eq 6–8. Naturally, the

$$\alpha = \frac{6}{5} \frac{V_0 - V_t}{V_0} \times 100\% \quad (9)$$

disproportionation proceeds also during the titration, a fact which was also neglected in estimating  $\alpha$ . Thus the titration provides only a semiquantitative estimate at best. So that all these difficulties could be overcome, studies involving spectrophotometric monitoring of the disproportionation are planned in our laboratory.

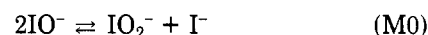
(ii) All of our results were interpreted on the assumption that the potential of the iodide-selective electrode is controlled by hypohalous acid alone, i.e., the effects of other corrosive species (iodous and iodic acids) are negligible. This assumption is discussed in detail later in this paper.

(iii) The initial jump of the potential observable on the curves in Figure 3a can be understood by considering the iodine(I) content of injected samples S1–S3. These samples contain iodine of several different oxidation states dissolved in 96% H<sub>2</sub>SO<sub>4</sub>. After injecting the samples into aqueous solutions, H<sub>2</sub>OI<sup>+</sup> is produced instantaneously from the iodine(I) species which causes the sudden rise of the potential. The iodine(III) species is converted to HIO<sub>2</sub>, the slow disproportionation of which to hypoiodous acid is responsible for the subsequent slow rise of the potential. The higher the [IO<sub>3</sub><sup>-</sup>]/[I<sub>2</sub>] ratio in the preparation of the sample the lower is its iodine(I) content (see Experimental Section), and consequently the lower the potential jump. The effect of the preparation ratio on the distribution of iodine among its different oxidation states becomes clear if one assumes the presence of a chemical equilibrium among the possible oxidation states in 96% H<sub>2</sub>SO<sub>4</sub>. By raising the I(V) content (as [IO<sub>3</sub><sup>-</sup>]) in the preparation, the equilibrium concentrations will be shifted toward decreasing iodine(I) and increasing iodine(III) concentrations.

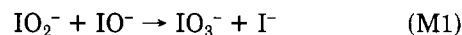
(iv) So that the mechanistic details of the disproportionation could be explored, a conversion of the measured

potential–time diagrams to [H<sub>2</sub>OI<sup>+</sup>] vs. time is necessary. In the case of the bromous acid decomposition the titration of HOBr after a practically complete disproportionation provided a reference point for calibration. An analogous method cannot be applied for the iodous acid in dilute acidic solutions because its decomposition is not complete on the time scale of the experiments, and H<sub>2</sub>OI<sup>+</sup> cannot be titrated separately either. In our previous study<sup>3</sup> this problem was not serious because the solutions used were ten times more concentrated than in the present work, resulting in a much higher rate of disproportionation, and thus a relatively small amount of undecayed HIO<sub>2</sub>. In lieu of direct calibration, the experimental calibration curve established previously at higher concentrations<sup>3</sup> was extrapolated. Since the relative position of the Ag<sup>+</sup> and H<sub>2</sub>OI<sup>+</sup> potential curves is fixed,<sup>3</sup> it is sufficient to measure the electrode response with silver ions in the concentration range of the desired extrapolation ([Ag<sup>+</sup>] = 10<sup>-5</sup> M, [H<sub>2</sub>SO<sub>4</sub>] = 0.15 M) immediately after each disproportionation experiment. Then the potential curve obtained during the disproportionation can be adjusted accordingly and [H<sub>2</sub>OI<sup>+</sup>]<sub>*t*</sub> can be calculated (right scale in Figure 3, b and d). This procedure eliminates the error caused by the possible day-to-day shift of the electrode potentials.

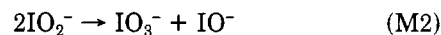
(v) Since iodine(III) has not been examined previously in aqueous acidic media, no experimental results are available for comparison. In alkaline media, however, some mechanisms were proposed for the disproportionation of iodite. According to Li and White,<sup>35</sup> after the rate-determining step



the iodite reacts with hypoiodite in the relatively fast reaction

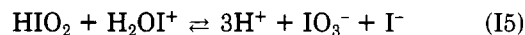


Haimovich and Treinin<sup>36</sup> reexamined the problem and concluded that after the rate-determining step (M0) the decomposition of iodite proceeds via (“mechanism II” in their terminology)



and (M1) (“mechanism I”) does not play a significant role in strongly basic solutions ([NaOH] = 4 M).

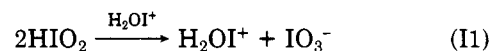
To describe the autocatalytic disproportionation of iodous acid in the acidic media used in our experiments (0.05 M < [H<sub>2</sub>SO<sub>4</sub>] < 0.15 M), we propose a mechanism with a rate-determining step (I5) analogous to (M1)



followed by the relatively fast reactions of (I2), or by the reaction scheme of (I3) and (I4). In both cases a net process (BL2) emerges resulting in an autocatalytic accumulation of hypoiodous acid



Naturally, omitting 1 mol of hypoiodous acid on both sides of (BL2), reaction I1 is obtained where H<sub>2</sub>OI<sup>+</sup> now plays the role of a catalyst.



(35) Li, C. H.; White, C. F. *J. Am. Chem. Soc.* 1943, 65, 335–9.

(36) Haimovich, O.; Treinin, A. *J. Phys. Chem.* 1967, 71, 1941–3.

TABLE III: Rate Constant of Reaction I5 as Function of Sulfuric Acid Concentration

$[\text{H}_2\text{SO}_4]/\text{M}$	0.15	0.10	0.05
$k_{15}/(\text{M}^{-1} \text{s}^{-1})$	$130 \pm 5$	$140 \pm 5$	$350 \pm 30$

Since  $\Gamma^-$  reacts very rapidly with  $\text{H}_2\text{OI}^+$ , the backward reaction in (I5) can be neglected. If the forward reaction is an elementary step, the rate of (I5) is given by

$$-d[\text{H}_2\text{OI}^+]/dt = k_{15}[\text{H}_2\text{OI}^+][\text{HIO}_2] \quad (10)$$

that integrates to

$$k_{15}[\text{HIO}_2]_0 t = \ln \frac{[\text{H}_2\text{OI}^+]}{[\text{H}_2\text{OI}^+]_0} + \ln \frac{[\text{HIO}_2]_0 - 2[\text{H}_2\text{OI}^+]_0}{[\text{HIO}_2]_0 - 2[\text{H}_2\text{OI}^+]_0} \quad (11)$$

where the subscript indicates initial values. Equation 11 was derived by the use of the stoichiometry of (I1) which gives the following material balance:

$$[\text{HIO}_2]_0 - [\text{HIO}_2] = 2([\text{H}_2\text{OI}^+] - [\text{H}_2\text{OI}^+]_0) \quad (12)$$

To calculate  $k_{15}$ , a linearization of the measured potential curves is possible. If the iodous acid concentration were constant during the disproportionation (e.g., by controlling its value by an external source), the second term on the right side of eq (11) would not appear, and the electrode potential  $E_t^*$  after the potential jump  $E_0$  would be naturally a linear function of time

$$E_t^* = \frac{59 \text{ mV}}{2.303} k_{15}[\text{HIO}_2]_0 t + E_0 \quad (13)$$

In reality, however,  $[\text{HIO}_2]$  decreases and the second term on the right side of (11) can be viewed as originating in the deviation from pseudo-first-order behavior. The corresponding deviation in potential response for nonlinearity is given by the correction term

$$\Delta E_c \equiv \frac{59 \text{ mV}}{2.303} \ln \frac{[\text{HIO}_2]_0 - 2[\text{H}_2\text{OI}^+]_0}{[\text{HIO}_2]_0 - 2[\text{H}_2\text{OI}^+]_0} \quad (14)$$

Thus, if the assumptions made are applicable, the experimentally measured potential  $E_t$  should be calculable from

$$E_t = E_t^* - \Delta E_c \quad (15)$$

if  $k_{1k}$  were known. But instead,  $E_t$  is known and  $\Delta E_c$  can be calculated, thus (15) can be used to obtain  $E_t^*$ , the slope of which, according to (13), yields  $k_{15}$ . The  $E_t^*$  ( $= E_t + \Delta E_c$ ) values computed at the points indicated as a function of time are depicted in Figure 3, b and d. The  $k_{15}$  values calculated from the slopes of the linear portions of the ( $E_t + \Delta E_c$ ) vs. time curves are listed in Table III. The curves are linear only in the initial period of the experiments because the disproportionation of  $\text{H}_2\text{OI}^+$  (that was neglected in the calculations) becomes significant at later stages of the reaction.

(vi) The rate of disproportionation of  $\text{HIO}_2$  decreases with increasing concentration of sulfuric acid (Table III, Figure 3d), just the opposite to the behavior of  $\text{HBrO}_2$ . If also  $\text{HIO}_2$  exists primarily in a protonated form, as does hypiodous acid,<sup>37</sup> one can understand the pH dependence of the rate of disproportionation if one assumes that only the unprotonated form can react with  $\text{H}_2\text{OI}^+$ . This would also explain the sudden rise of the rate in the most dilute (0.05 M) sulfuric acid solution where the fraction of the unprotonated iodous acid should be higher, and the uncatalyzed disproportionation may play an increasingly important role in addition to the autocatalytic route.

TABLE IV: Estimated Rate Constants  $k_{11}$  of Reaction I1

ref	32	34	38	this work ( $k_{11}$ ) <sub>max</sub> <sup>a</sup>
temp/°C	50	25	25	24
medium	perchloric acid	perchloric acid	perchloric acid	sulfuric acid
$[\text{H}^+]/\text{M}$	0.05	0.056	0.057	0.05, 0.10, 0.15
$k_{11}/(\text{M}^{-1} \text{s}^{-1})$	$5.56 \times 10^7$	$6 \times 10^5$	45.3	5.4, 2.2, 2.0

<sup>a</sup> This work can provide an upper limit only.

Haimovich and Treinin's results<sup>36</sup> suggest that such a change in mechanism (from "mechanism I" to "mechanism II") may occur with rising pH.

*Possible Sources of Error.* Since the disproportionation of iodous acid is slow, no special attention had to be paid to the rate of mixing of the reagents. The most important source of error was the nonideal behavior of the iodide-selective electrode in the range of low concentrations used. Here, deviations from Nernstian response and "memory" effects caused uncertainties in the calibration curve. An interesting beneficial memory effect is worth mentioning: after treating the electrode with iodine solutions (as it happens in titrations of  $\text{H}_2\text{OI}^+$  with  $\text{I}_2$ ), an approximately Nernstian response could be observed for  $\text{Ag}^+$  and  $\text{H}_2\text{OI}^+$  in the concentration range where a non-Nernstian response was caused by the presence of oxygen beforehand. Since the estimation of the systematic errors would require a separate study, the uncertainties in Table III are given as standard deviations, indicating only the reproducibility of the data.

*Comparison with Previous Results. An Estimate of  $k_{11}$ .* The disproportionation of  $\text{HIO}_2$  plays an important role in the mechanistic schemes suggested for the BL and BR reactions. It is interesting to note that recently Noyes and Furrow<sup>38</sup> and DeKepper and Epstein<sup>34</sup> have proposed identical schemes for the BR reaction, with a major difference in the value of  $k_{11}$  only. In spite of the lack of experimental data, several, greatly different estimates have been used in the literature for the rate constant of reaction I1 (see Table IV). Although, a different mechanism is suggested for the disproportionation of  $\text{HIO}_2$  by our results, the data can be used to estimate the *upper limit* of the rate constant ( $k_{11}$ )<sub>max</sub>, if one assumes that the measured rate of the decomposition is exclusively due to the mechanism proposed by the above authors, namely, a direct reaction according to (I1). Then, our expression 10, now specified for the initial rate  $r_0$  of (I5), must be set identical with the rate expression of (I1)

$$r_0 = k_{15}[\text{H}_2\text{OI}^+]_0[\text{HIO}_2]_0 \equiv 2(k_{11})_{\text{max}}[\text{HIO}_2]_0^2 \quad (16)$$

From (16), ( $k_{11}$ )<sub>max</sub> can be expressed as

$$(k_{11})_{\text{max}} = k_{15}[\text{H}_2\text{OI}^+]_0/2[\text{HIO}_2]_0 \quad (17)$$

The values calculated are displayed in Table IV.

*Observations on the Reactions of  $\text{HOI}_2$  with  $\text{I}_2$  and  $\Gamma^-$ .* A Lotka-Volterra Model for the BR Reaction. The reaction of  $\Gamma^-$  with  $\text{HIO}_2$  (I2) was too fast to be followed potentiometrically, thus one can estimate that  $k_{12} > 10^6 \text{ M}^{-2} \text{ s}^{-1}$ . Iodine appears already during the mixing of the reagents, and only the slower reaction between  $\text{I}_2$  and  $\text{HIO}_2$  can be recorded (see the titration curves in Figure 3c).

Similarly to the case of bromous acid, we attempted to obtain information about reaction I4, by introducing  $\text{I}_2$  prior to the instantaneous production of  $\text{HOI}_2$ . Subse-

(37) Bell, R. P.; Gelles, E. *J. Chem. Soc.* 1951, 2734-40.

(38) Noyes, R. M.; Furrow, S. D. *J. Am. Chem. Soc.* 1982, 104, 45-8.

TABLE V: Effect of the Initial Iodine Concentration  $[I_2]_0$  on the Competitive Processes I1 and I4

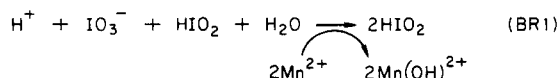
$[I_2]_0/[M]$	0	$4 \times 10^{-5}$	$8 \times 10^{-5}$	$2 \times 10^{-4}$
$t/\text{min}$	25	3	2.5	1.5
$V_t/\text{cm}^3$ <sup>a</sup>	0.75	1.60	2.00	2.30
$R$ <sup>b</sup>	0.3 <sup>c</sup>	3.0	5.2	7.9

<sup>a</sup>  $V_t$  is volume of titrant ( $10^{-3}$  M KI) required after  $t$  minutes of reaction (at the maximum of the electrode potential). <sup>b</sup>  $R \equiv [H_2OI^+]$  produced in (I4)/ $[H_2OI^+]$  produced in (I1). With reference to the stoichiometry of reactions I1 and I4, this ratio is also given by  $R = (y - 1)/(1 - y/6)$ , where  $y = 2[H_2OI^+]/[HIO_2]_0 = V_t/0.6 \text{ cm}^3$ . The  $0.6 \text{ cm}^3$  is the volume of titrant that would be needed if only reaction I1 would take place. <sup>c</sup> As it was pointed out the  $R$  values can be regarded as assumptions only. E.g., in the case of  $[I_2]_0 = 0$ ,  $R$  should be equal to zero instead of 0.3 indicated by the first column. The error is caused again by the nonzero iodous acid content at the time of titration.

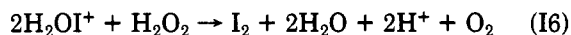
quently, when the electrode potential reached its maximum (corresponding to the maximum concentration of  $H_2OI^+$ ), the solution was titrated with  $10^{-3}$  M KI. The results of these preliminary experiments are given in Table V. As it was pointed out previously, the results of the titrations cannot be evaluated exactly, because at the time of titration the solution still contains a small unknown amount of  $HIO_2$ . Nevertheless, by assuming that the titrant was solely used for  $H_2OI^+$  produced in reactions I1 and I4, from their stoichiometry one can estimate the ratio  $R$  in which these two reactions contribute to the final total amount of  $H_2OI^+$ .

These results show qualitatively that process I4 is important and it can compete with (I1) even at relatively low iodine concentrations. Similarly to the case of (B4) it is not clear to us that process I4 goes via the hydrolysis of iodine followed by a rereaction between iodide and iodous acid or that elementary iodine can react directly with iodous acid providing another channel for (I4). Regardless of the unknown elementary steps involved, reaction I4 may play an important role in the BR reactions too where elementary iodine appears and disappears periodically in the course of the reaction.

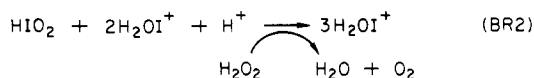
To explain the chemical oscillations in the BR reactions, Noyes and Furrow<sup>38</sup> and DeKepper and Epstein<sup>34</sup> independently proposed the following autocatalytic process



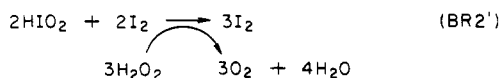
Now (I4) and the reaction between hypoiodous acid and hydrogen peroxide



((I6) is also part of the Noyes-Furrow-DeKepper-Epstein mechanism) can form a second autocatalytic step (BR2) in an analogous way to (BZ2)



or combining  $2 \times$  (I4) with  $3 \times$  (I6) results in



(BR2') is clearly analogous to (BZ2'). Therefore, similarly to the BZ systems, (BR1) and (BR2) or (BR2') can form a Lotka-Volterra<sup>29,30</sup> type "core"<sup>31</sup> for the BR systems. Since the autocatalytic process (BL2) may also be part of

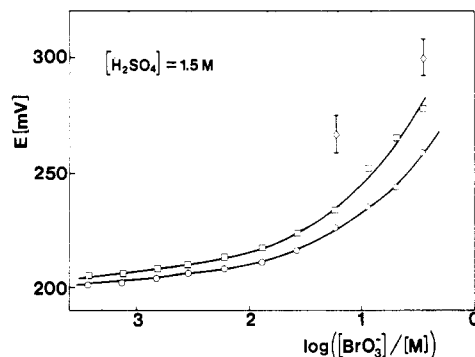


Figure 4. Potential response of the bromide-selective electrode for acidic bromate  $[H_2SO_4] = 1.5$  M. Hydrodynamic conditions: (i) strong stirring was applied and the stirrer was close to the electrode; the measured points are marked by (O). (ii) slow stirring, the stirrer was far from the electrode ( $\square$ ). (iii) unstirred solution ( $\diamond$ ).

the overall scheme, we can find an unexpectedly large number of autocatalytic processes in the Briggs-Rauscher reaction.

III. Potential Response of the Bromide-Selective Electrode for Acidic Bromate (Figure 4). Potential changes of the bromide-selective electrode caused by acidic bromate was investigated lately by Ganapathisubramanian and Noyes.<sup>39</sup> We examined the corrosive effect of bromate in 1.5 M sulfuric acid media containing malonic acid as well. Malonic acid was applied partly because the real BZ systems usually contain some organic substrate which can be brominated,<sup>7,40</sup> partly because acidic bromate is usually contaminated by hypobromous acid traces. The contamination can be removed by malonic acid via bromination and the corrosion potential established by acidic bromate can be studied separately. The corrosion of bromide-selective electrode by acidic bromate is a typical slow corrosive process. There are two characteristic features in Figure 4 indicating that (i) the measured potential depends on the stirring rate and (ii) the slope of the potential-log  $[BrO_3^-]$  curve (measured at a given stirring rate) is much less than the Nernstian  $\sim 59$  mV and it is close to  $\sim 15$  mV predicted by the theory of slow corrosive processes (cf. eq 40). The higher slopes of the curves at high bromate concentrations are probably due to a direct reaction of the corrosive agent with the electrode material. Also the long time (20–30 min) necessary to achieve a steady potential at high concentrations suggests that some process occurring in the solid phase is responsible for the slow change of the potential. (No diffusion process in the boundary layer can have a relaxation time longer than a few seconds.<sup>41</sup>)

If the concentration of bromate was less than  $10^{-4}$  M (like the concentrations of bromate formed in the experiments in the disproportionation of bromous acid, see Figure 2) its effect on the electrode potential was under the detection limit.

Potential Response of the Iodide-Selective Electrode for Acidic Iodate and Oxygen. As all the measured values depend on the rate of stirring and somewhat also on the history of the electrode, we report qualitative or semi-quantitative results only.

In solutions saturated with air very little or no corrosive effect of acidic iodate ( $[H_2SO_4] = 0.15$  M) can be observed because it is masked by the corrosion due to oxygen.<sup>3,42</sup> In

(39) Ganapathisubramanian, N.; Noyes, R. M. *J. Phys. Chem.* 1982, 86, 3217–22.

(40) Noszticzius, Z. *Magy. Kem. Foly.* 1979, 85, 330–1.

(41) Morf, W. E.; Lindner, E.; Simon, W. *Anal. Chem.* 1975, 47, 1596–601.

(42) Kontoyannakos, J.; Moody, G. J.; Thomas, J. D. R. *Anal. Chim. Acta* 1976, 85, 47–53.

an air-saturated solution of 0.15 M sulfuric acid the electrode potential is about 230 mV (quiescent liquid) or about 170 mV (strongly agitated solution). This "stirring effect" can be nearly eliminated by bubbling nitrogen through the solution under stirring for about 1 h. Thereafter, an electrode potential of about 150 mV can be measured and a discontinuation of stirring causes only a relatively small and slow change of the potential. (It is rather probable that at least part of the corrosive oxygen is chemisorbed on the electrode surface and its complete removal would require an even longer time.)

Corrosion potentials and also a "stirring effect" in acidic iodate can be observed separately in oxygen-free 0.15 M sulfuric acid solutions. In this case curves similar to the ones in Figure 4 can be obtained but their slopes are only a few millivolts/log concentration. Also no signs of heterogeneous reactions between the solid phase and the acidic iodate were detected.

Concentration changes of iodate in the range of  $10^{-5}$ – $10^{-4}$  M do not produce measurable changes in the electrode potential. Consequently corrosion potentials due to acidic iodate during the disproportionation of iodous acid can be neglected.

### Theoretical Section

*Application of CPT to Slow Corrosive Processes.* In the case of relatively fast corrosive processes studied in our previous work<sup>3</sup> it was assumed that all the chemical reactions take place within a narrow "reaction zone" close to the surface of the electrode (see Figure 6), the width of which was only a small fraction of the stagnant boundary layer thus it could be neglected. The rate of the whole process was controlled by the diffusion of the corrosive agent (e.g., hypobromous acid) through the boundary layer to the surface of the electrode (e.g., silver bromide electrode) where its concentration was considerably lower than in the bulk of the solution. The depletion was relatively important compared to the low bulk concentrations ( $10^{-6}$ – $10^{-4}$  M) of the corrosive agent.

In this paper we deal with slow corrosive processes which display a different behavior in many respects. For example, acidic bromate can affect the potential of the bromide-selective electrode only in relatively high ( $10^{-3}$ – $10^{-1}$  M) concentrations because the bromide–bromate reaction is much slower than the bromide–hypobromous acid reaction. Consequently, the concentration decrease of the corrosive agent in the boundary layer can be neglected here compared to the higher concentrations existing both in the bulk and in the boundary layer (Figure 5). Furthermore, the whole boundary layer becomes a "reaction zone" now provided the corrosive reaction takes place in the liquid phase and it is not a heterogeneous one.

In the following the halate–halide reaction will be discussed as a special example for a slow corrosive process. (The results can easily be generalized to include other cases.) In general, the rate law of the corrosive reaction (CR3) can be written in this case as

$$r_x = k_c[\text{XO}_3^-][\text{X}^-] \quad (18)$$

where  $r_x$  is defined as the rate of halide consumption. The concentration profiles of the different species in the boundary layer are depicted in Figure 5. As the electrode potential depends on the interfacial silver ion concentration  $[\text{Ag}^+]_i$  generated by the corrosion process, the aim of the subsequent derivation is to find an expression for  $[\text{Ag}^+]_i$  as a function of the corrosive halate concentration in the bulk  $[\text{XO}_3^-]_b$ , i.e.

$$[\text{Ag}^+]_i = F([\text{XO}_3^-]_b) \quad (19)$$

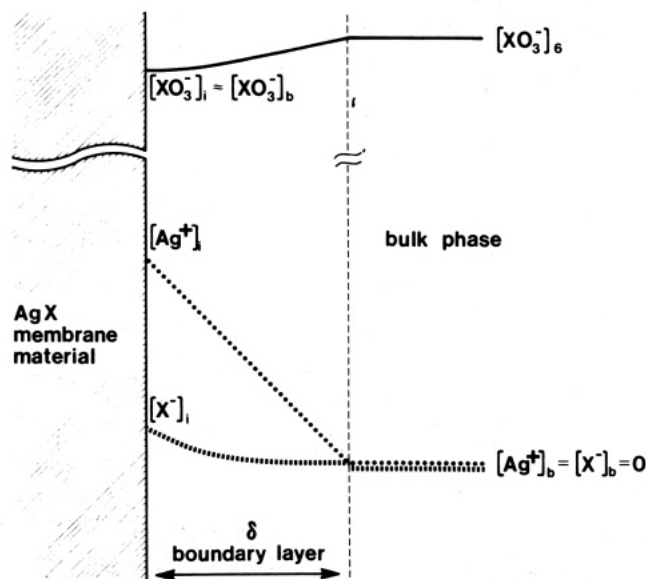


**Figure 5.** Schematic representation of the concentration profiles in the vicinity of the electrode surface in the case of "slow" corrosive processes. The subscripts indicate interfacial (i) and the bulk (b) values of the concentrations. The diffusion processes and the corrosive reaction take place in the Nernst boundary layer of thickness  $\delta$ , whereas the concentrations in the bulk phase are considered to be uniform.

where  $F$  is the desired formula, and the following assumption will be used:

$$[\text{XO}_3^-]_i \approx [\text{XO}_3^-]_b \equiv [\text{XO}_3^-] \quad (20)$$

From a theoretical point of view, the applicability of (20) can be regarded as the most characteristic feature of a "slow" corrosive process.

The current densities of the silver and the halide ions ( $J_{\text{Ag}^+}$  and  $J_{\text{X}^-}$ ) are given by

$$J_{\text{Ag}^+} = -D_{\text{Ag}^+}(d[\text{Ag}^+]/dx) \quad (21)$$

$$J_{\text{X}^-} = -D_{\text{X}^-}(d[\text{X}^-]/dx) \quad (22)$$

according to Fick's law.  $D_{\text{Ag}^+}$  and  $D_{\text{X}^-}$  are the diffusion coefficients of the relevant species and  $x$  is the distance measured from the surface of the electrode. At steady state

$$J_{\text{Ag}^+} = \text{constant} = D_{\text{Ag}^+}([\text{Ag}^+]_i/\delta) \quad (23)$$

and

$$d(J_{\text{X}^-})/dx = r_x \quad (24)$$

Equation 24 can be written in a dimensionless form by introducing the so-called Thiele modulus<sup>43</sup>  $h_T$  defined as

$$h_T^2 \equiv \frac{k_c[\text{XO}_3^-]\delta^2}{D_{\text{X}^-}} \quad (25)$$

Then, with (18), (20), and (22) we have

$$\frac{d^2[\text{X}^-]}{d(x/\delta)^2} = h_T^2[\text{X}^-] \quad (26)$$

The solution of (26), with the boundary conditions of Figure 5, gives

$$[\text{X}^-] = [\text{X}^-]_i \sinh [h_T(1 - x/\delta)]/\sinh h_T \quad (27)$$

the concentration distribution of the halide ions in the boundary layer.

(43) Hill, C. G. Jr. "An Introduction to Chemical Engineering Kinetics and Reactor Design"; Wiley: New York, 1977; pp 440, 444.

With the aid of (22) and (27) the current density of the halide ions on the surface of the electrode ( $J_{X^-}_i$ ) can be expressed as

$$(J_{X^-})_i = D_{X^-}([X^-]_i/\delta)\eta \quad (28)$$

where

$$\eta = h_T/\tanh h_T \quad (29)$$

On the surface of the silver halide electrode two further relations hold: the solubility equilibrium

$$[Ag^+]_i[X^-]_i = K_s \quad (30)$$

and the constraint of zero electric current density

$$(J_{X^-})_i = (J_{Ag^+})_i \quad (31)$$

Using (21), (28), (29), (30), and (31) we obtain

$$[Ag^+]_i = (D_{X^-}/D_{Ag^+})K_s\eta \quad (32)$$

With respect to (32), two limiting cases can be considered. If the concentration of the corrosive halate  $[XO_3^-]$  is so small that

$$h_T < 0.5 \quad (33)$$

is satisfied (cf. (25)) then regarding (29)

$$\eta \approx 1 \quad (34)$$

and with the approximation

$$D_{X^-}/D_{Ag^+} \approx 1 \quad (35)$$

the interfacial silver ion concentration can be expressed as

$$[Ag^+]_i \approx K_s^{1/2} \quad (36)$$

In other words if the concentration of the corrosive agent is so low that (36) is valid no measurable corrosion effect can be observed. On the other hand, if the concentration of the corrosive agent is high enough to satisfy the inequality

$$h_T > 2 \quad (37)$$

then the approximation

$$\eta \approx h_T \quad (38)$$

can be applied and for the interfacial silver ion concentration we get the following expression:

$$[Ag^+]_i \approx (K_s h_T)^{1/2} \quad (39)$$

(cf. (32), (35), and (38)). The measured electromotive force as a function of the halate concentration has the following form:

$$E = E_0 + \frac{59 \text{ mV}}{2} \log(K_s \delta) + \frac{59 \text{ mV}}{4} \log \frac{k_c [XO_3^-]}{D_{X^-}} \quad (40)$$

*Interpretation of the Experimental Results by CPT.* Equation 40 predicts the experimentally observed stirring effect: the smaller the stirring rate the higher corrosion potential can be measured as the width of the stagnant boundary layer  $\delta$  increases, decreasing the hydrodynamic flow. Also the non-Nernstian response for the corrosive  $[XO_3^-]$  ( $\sim 15$  mV/concentration decade) is in qualitative agreement with (40). To make a quantitative comparison is not easy because the experimental values are uncertain exactly because of the stirring effect and in the case of iodate there are some theoretical problems as well regarding the different rate laws for the Dushman reaction.<sup>40</sup> Nevertheless, a semiquantitative comparison is possible by using the different rate laws for (CR3). The rate law for bromate<sup>20</sup> is given by

$$d[\text{BrO}_3^-]/dt = -(2.1 \text{ M}^{-3} \text{ s}^{-1})[\text{H}^+]^2[\text{BrO}_3^-][\text{Br}^-] \quad (41)$$

For iodate there are several expressions<sup>44</sup> even for low iodide concentrations<sup>45</sup> where terms containing  $[\text{I}^-]^2$  can be disregarded. E.g., according to Abel and Hilferling<sup>46</sup>

$$d[\text{IO}_3^-]/dt = -(2.4 \times 10^4 \text{ M}^{-3} \text{ min}^{-1})[\text{H}^+]^2[\text{IO}_3^-][\text{I}^-] \quad (42)$$

or according to Connick and Hugus<sup>47</sup>

$$d[\text{IO}_3^-]/dt = -(1.1 \times 10^6 \text{ M}^{-4} \text{ min}^{-1})[\text{H}^+]^3[\text{IO}_3^-][\text{I}^-] \quad (43)$$

The  $k_c$  value in (18) for  $\text{BrO}_3^-$  is  $\sim 10 \text{ M}^{-1} \text{ s}^{-1}$  calculated from (41) ( $[\text{H}^+] = 1.5 \text{ M}$  and, as  $k_c$  refers to the bromide consumption in (18) by definition, a factor of 2 was used because 1 mol of bromate removes 2 mol of bromide in the presence of malonic acid). For  $\text{IO}_3^-$ ,  $k_c = 45 \text{ M}^{-1} \text{ s}^{-1}$  or  $309 \text{ M}^{-1} \text{ s}^{-1}$  calculated from (42) or (43), respectively ( $[\text{H}^+] = 0.15 \text{ M}$  and, as  $k_c$  refers to the iodide consumption, here a factor of 5 was used). From our measurements (Figure 1 in ref 3, titration curves of acidic iodate by iodide)  $k_c \approx 400 \text{ M}^{-1} \text{ s}^{-1}$  can be estimated.

Regarding (25) and (37) we can expect a measurable corrosion effect when the halate concentration exceeds a critical value  $[XO_3^-]_c$

$$[\text{XO}_3^-]_c = \frac{4D_{X^-}}{k_c \delta^2} \quad (44)$$

The critical concentration for bromate, based on (41) and (44), is

$$[\text{BrO}_3^-]_c \approx 8.5 \text{ M} \quad (45)$$

For iodate we can give a range only because of the uncertainty in the  $k_c$  value

$$[\text{IO}_3^-]_c \approx 0.2\text{--}1.7 \text{ M} \quad (46)$$

In the derivation of (45) and (46) the following approximations were made:  $D_{X^-} \approx 10^{-5} \text{ cm}^2/\text{s}$ ,  $\delta \approx 10^{-3} \text{ cm}$ . As Figure 4 shows the acidic bromate can produce a corrosion potential in concentrations much below the expected  $\sim 8.5 \text{ M}$ . Also the magnitude of the observed effect is too large. There are two possibilities to explain this unexpected behavior: (i) the rate law is different at high bromate concentrations; or (ii) there is a heterogeneous reaction between the solid state bromate and the dissolved bromate in this concentration region.

Corrosion potentials established by acidic iodate can be explained theoretically within the experimental error. Apparently, no considerable heterogeneous reaction takes place between solid silver iodide and acidic iodate in agreement with earlier investigators.<sup>45</sup>

*Transition from "Fast" to "Slow" Corrosive Processes. An Upper Limit for  $k_{B2}$  and  $k_{I2}$ .* Rather simple theories for fast and slow corrosive processes are available now. Nevertheless, we must keep in mind that these are limiting cases giving good approximations only if properly applied. Therefore, a criterion is needed on the basis of which it can be decided whether a corrosive process is to be regarded as "fast" or "slow". It can be shown (see Appendix

(44) Liebhafsky, H. A.; Roe, G. M. *Int. J. Chem. Kinet.* 1979, 11, 693-703.

(45) Furuichi, R.; Matsuzaki, S.; Simic, R.; Liebhafsky, H. A. *Inorg. Chem.* 1972, 11, 952-55.

(46) Abel, E.; Hilferling, K. *Z. Phys. Chem.* 1928, 136, 186.

(47) Connick, R. E.; Hugus, Z. Z., Jr. Brookhaven Conference Report BNL-C-8, Chemical Conference No. 2, 1948, p 164.

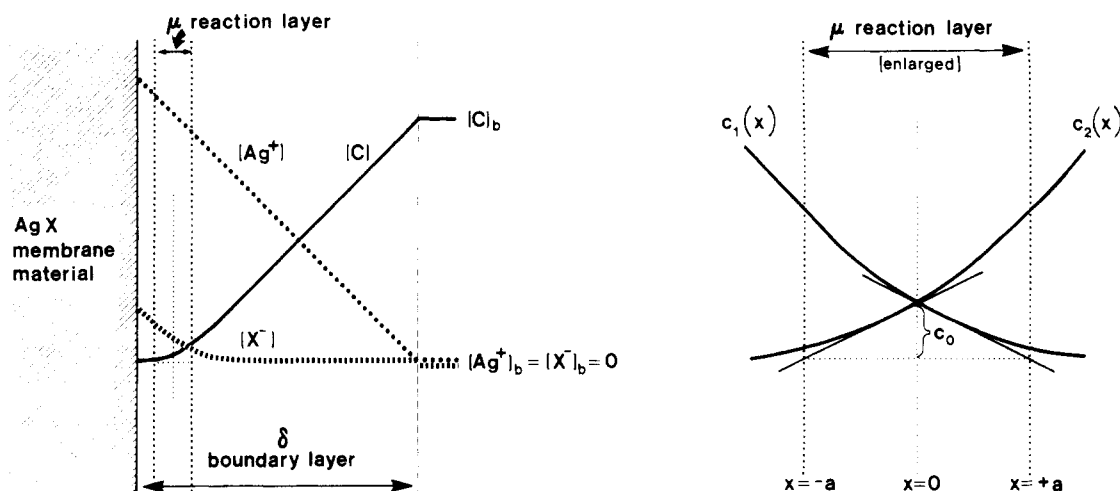


**Figure 6.** Schematic representation of the concentration profiles within the boundary and reaction layers. To calculate  $c_1(x)$  and  $c_2(x)$  as an example it was assumed that  $D_{X^-}/D_{C_2} < 1$  (cf. (A2)).

and Figure 6) that the thickness of the reaction layer " $\mu$ " where a relatively fast reaction takes place close to the surface of the electrode can be estimated by

$$\mu \approx 2.5 \left( \frac{\delta D_{X^-}}{[C]_b k_c} \right)^{1/3} \quad (47)$$

where  $[C]_b$  is the concentration of the corrosive agent C in the bulk of the solution and  $k_c$  is the rate constant in the generalized rate expression

$$r_x = k_c [X^-][C] \quad (48)$$

Again,  $r_x$  is the rate of halide consumption. With the assumption used in the previous section ( $\delta \approx 10^{-3}$  cm,  $D_{X^-} \approx 2 \times 10^{-5}$  cm<sup>2</sup>/s) for the thickness of the reaction layer, e.g., with  $[\text{HOBr}] = 10^{-5}$  M ( $[\text{H}^+] = 1.5$  M,  $k_c = k_{B3}[\text{H}^+]$ ,  $k_{B3} = 8 \times 10^9$  M<sup>-2</sup> s<sup>-1</sup><sup>20</sup>) we get  $\mu \approx 1.4 \times 10^{-4}$  cm and with  $[\text{H}_2\text{OI}^+] = 10^{-5}$  M ( $k_c = k_{I3}$ ,  $k_{I3} = 4.5 \times 10^{10}$  M<sup>-1</sup> s<sup>-1</sup><sup>49</sup>)  $\mu \approx 0.9 \times 10^{-4}$  cm. That is, in both cases the inequality

$$\mu < 0.2\delta \quad (49)$$

is satisfied. For higher hypohalous concentrations  $\mu$  is even smaller. As the experimental results show,<sup>3</sup> the mathematical model developed for fast reactions gave a rather good approximation in these cases. On the other hand, if

$$\mu > \delta \quad (50)$$

the fast corrosion model is meaningless (the reaction layer cannot be thicker than the boundary layer) and the model describing the slow corrosive processes should be used. Reversely, if a corrosive process is found to be slow we can calculate an upper limit for its rate on the basis of (50) because combining (47) and (50) yields

$$2.5 \left( \frac{\delta D_{X^-}}{[C]_b k_c} \right)^{1/3} > \delta \quad (51)$$

$$k_c < \frac{16D_{X^-}}{[C]_b \delta^2} \quad (52)$$

This idea can be applied for the estimation of  $k_{B2}$  and  $k_{I2}$ . As it was pointed out previously reactions B2 and I2 were too fast to follow potentiometrically. We could esti-

mate only a lower limit of  $10^6$  M<sup>-2</sup> s<sup>-1</sup> for their rate constants. Now based on (52) also an upper limit can be evaluated if we can show that the corrosion process caused by halous acids (denoted by (CR2) in the Introduction) is a slow one. ((B2) and (I2) are rate-determining steps of the overall process CR2.)

Our experiments with halous acids indicate indeed that (CR2) is certainly not a fast corrosive process. Namely, during the disproportionation of bromous and iodous acids an increasing potential of the bromide- and iodide-selective electrodes were observed (cf. Figures 2 and 3). As the final concentration of the hypohalous acids responsible for (CR1) is only half of the original halous acid concentration, and (CR2) consumes three times more halide ions than (CR1), the halous acids should produce a corrosion potential of  $59 \text{ mV} \times \log(2 \times 3) = 45 \text{ mV}$  higher than the hypohalous acids formed in their disproportionation, if (CR2) were a fast process. In that case the disproportionation would result in a falling potential instead of the observed rise. Thus, we can conclude that (CR2) unlike (CR1) is a slow corrosive process.

Now if we apply the above-mentioned approximations for  $\delta$  and  $D_{X^-}$ , and as the halous acid concentration in both cases (Br, I) was  $[C]_b \geq 2 \times 10^{-5}$  M, (52) gives

$$k_c < 16 \times 10^{-6} \text{ M}^{-1} \text{ s}^{-1} \quad (53)$$

Now for bromous acid ( $[\text{H}^+] \approx 1.5$  M,  $k_c = 3k_{B2}[\text{H}^+]$ ) and for iodous acid ( $[\text{H}^+] \approx 0.15$  M,  $k_c = 3k_{I2}[\text{H}^+]$ ) the estimated upper limits are  $k_{B2} < 4 \times 10^6$  M<sup>-2</sup> s<sup>-1</sup> and  $k_{I2} < 4 \times 10^7$  M<sup>-2</sup> s<sup>-1</sup>. For comparison we list the following theoretical estimates reported in the literature:

$$k_{B2} = 2 \times 10^9 \text{ M}^{-2} \text{ s}^{-1} \quad [\text{ref } 20]$$

$$k_{I2} = 2 \times 10^9 \text{ M}^{-2} \text{ s}^{-1} \quad [\text{ref } 33]$$

$$k_{I2} = 2 \times 10^{10} \text{ M}^{-2} \text{ s}^{-1} \quad [\text{ref } 34]$$

as (B2) and (I2) play an important role in the present theories of the BZ, BL, and BR reactions.<sup>20,32,34,38</sup>

## Conclusion

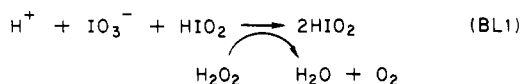
1. *The corrosive processes can be classified as "fast" and "slow" and relatively simple mathematical models can be found to describe the limiting cases. A characteristic feature of corrosion potentials established by slow processes is a non-Nernstian behavior and they depend on the rate of stirring. The reaction layer concept can be successfully applied to classify the two different types of corrosive processes.*

(48) Vetter, K. J. "Electrochemical Kinetics"; Academic Press: New York, 1967; pp 188-98.

(49) Grant, J. L.; DeKepper, P.; Epstein, I. R.; Kustin, K.; Orban, M. *Inorg. Chem.*, in press.

Since relatively fast reactions may be categorized as "slow" ones, this fact can be used to estimate an upper limit for the rate constant of such corrosive reactions as in the case of halous acid-halide ion reactions.

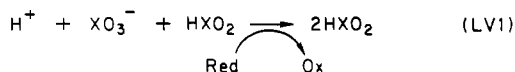
2. Our most important finding is that *there are at least two consecutive autocatalytic processes in all of the known halate-driven oscillators*. To complete the set of autocatalytic processes we have to mention



which is in fact an uncatalyzed variant of (BR1). (In (BR1) the net process BL1 is catalyzed by the  $\text{Mn}^{2+}/\text{Mn}^{3+}$  redox couple.)<sup>34,38</sup>

As the BL reaction takes place at higher temperatures than the BR reaction, it is probable that (BL1) has only a secondary importance in the BR reaction. Nevertheless, it is interesting to point out that in a BR system four autocatalytic processes may occur: (BL1), (BL2), (BR1), and (BR2). Also a BL system may contain three autocatalytic processes, namely, (BL1), (BL2), and (BR2).

Thus, one can write a Lotka-Volterra scheme for the halate-driven oscillators ( $X = \text{Br}, \text{I}$ ) as an autocatalytic process



(where  $\text{Red} \rightarrow \text{Ox}$  denotes various auxiliary reactions; see (BL1), (BZ1), and (BR1)) followed by a second autocatalytic process (LV2), which can have different forms (see (BL2), (BZ2), (BZ2'), (BR2), and (BR2')). The last step of the LV scheme is the removal of an intermediate from the system (LV3). This can be a chemical reaction (e.g., removal of HOBr by malonic acid) or a physical process as well (e.g., removal of  $\text{Br}_2$  by an inert gas stream<sup>26</sup>).

It is interesting to note that a recently discovered new family of chlorite-based chemical oscillators may also contain more than one autocatalytic processes.<sup>50,51</sup>

3. The Lotka-Volterra model has often been criticized because it executes conservative oscillations without a limit cycle, and it is structurally unstable against the introduction of any other reaction involving its two intermediates. It was shown, however,<sup>31,52,53</sup> that both problems can be overcome by introducing a third intermediate into the LV system. In the case of the halate-driven oscillators the different oxidation levels of the halogen—the halous and hypohalous acids, the elementary halogens, and halide ions—provide four intermediates. Even if an equilibrium relationship due to fast reactions among the +1, 0, and -1 oxidation states decreases the number of the independent variables by one, we can still have the required three intermediates. (Naturally, free radicals and other exotic—and very reactive—halogen compounds can be present as further intermediates, but they are only "flow through intermediates" which are not able to accumulate above a trace level in a real oscillating system.) In this respect, it is important that according to our results the *disproportionation of halous acids and the halous acid-halide ion reactions are much slower processes than it was assumed*

previously. Therefore, halous acid intermediates can occur in higher concentrations as it was proposed by Noyes and Furrow<sup>38</sup> in the case of BR reaction.

4. In the real oscillating systems there is a mixture of corrosive agents. Also, most of the previous investigators used commercial ion-selective electrodes containing silver halide-silver sulfide membranes. To achieve our final goal—the interpretation of the potential oscillations of these electrodes in oscillating reactions—we shall discuss these problems in a subsequent, concluding paper.<sup>54</sup>

*Acknowledgment.* This work was partially supported by the R. A. Welch Foundation and the Organized Research Fund of UTA. Acknowledgment is made to the donors of the Petroleum Research Fund, administered by the American Chemical Society, for partial support of this work. The authors are grateful to Professor H. D. Försterling and Dr. H. J. Lamberz for providing  $\text{NaBrO}_2$  solution samples and M. W. Lutes for technical assistance.

## Appendix

*Thickness  $\mu$  of the Reaction Layer. Derivation of Eq 47.* The reaction layer concept was developed to study fast chemical reactions by polarographic techniques.<sup>55</sup> A thin "reaction layer" of thickness  $\mu$  was defined similar to the much thicker diffusion layer  $\delta$ . It is assumed that most of the investigated chemical reaction takes place in this layer. In fact, as a convenient simplification, the rate of the reaction in most cases is regarded to be constant within the reaction layer and zero outside of that layer. In our case the two reacting species—the halide ion  $\text{X}^-$  and the corrosive agent C—diffuse against each other and react according to the generalized reaction of corrosion



close to the silver halide membrane. If the reaction is fast enough it is reasonable to assume, here too, that a narrow "reaction zone" exists in the vicinity of the electrode outside of which the rate of the reaction is negligible. (In the theory developed for fast corrosive processes<sup>3,56</sup> the thickness of this layer was neglected, as a good approximation. On the other hand, when the corrosive process is slow the whole diffusion layer can be regarded as a reaction layer.) A qualitative picture of the stationary concentration profiles can be seen in Figure 6. In steady state the following system of differential equations holds (cf. (CR), (48), (24)):

$$D_{\text{X}^-} \frac{d^2[\text{X}^-]}{dx^2} = k_c[\text{X}^-][\text{C}] \quad D_c \frac{d^2[\text{C}]}{dx^2} = \frac{k_c}{z}[\text{X}^-][\text{C}] \quad (\text{A1})$$

Let us introduce the following new variables:

$$c_1 \equiv \frac{D_{\text{X}^-}}{D_c} \frac{[\text{X}^-]}{z} \quad c_2 \equiv [\text{C}] \quad (\text{A2})$$

With (A2), (A1) can be transformed into a symmetrical form

$$D_{\text{X}^-} \frac{d^2c_1}{dx^2} = k_c c_1 c_2 \quad D_{\text{X}^-} \frac{d^2c_2}{dx^2} = k_c c_1 c_2 \quad (\text{A3})$$

(See also Figure 6.) Since this differential equation system (A3) has no analytical solution<sup>57</sup> we shall use the reaction

(50) DeKepper, P.; Epstein, I. R.; Kustin, K. *J. Am. Chem. Soc.* 1981, 103, 2133-4.

(51) Dateo, C. E.; Orban, M.; DeKepper, P.; Epstein, I. R. *J. Am. Chem. Soc.* 1982, 104, 504-9.

(52) Gray, B. F.; Aarons, L. *J. Faraday Symp. Chem. Soc.* 1974, 9, 129-36.

(53) Hofbauer, J. *Nonlinear Analysis* 1981, 5, 1003-7.

(54) Noszticzius, Z.; Noszticzius, E.; Schelly, Z. A., manuscript in preparation.

(55) Strehlow, H. In "Techniques of Chemistry"; Hammes, G. G., Ed.; Wiley: New York, 1974; Vol. IV, 3rd ed, pp 288-94.

(56) Noszticzius, Z. *Acta Chim. Acad. Sci. Hung.* 1981, 106, 347-57.

(57) Danckwerts, P. V. "Gas Liquid Reactions"; McGraw-Hill: New York, 1970; pp 115-6.

layer concept as an approximation. Let us introduce a frame of reference where the two transformed concentrations are equal at  $x = 0$

$$c_1(0) = c_2(0) \equiv c_0 \quad (\text{A4})$$

Now according to the reaction layer concept

$$c_1 c_2 \approx c_0^2 = \text{constant} \quad (\text{A5})$$

holds within the layer. The first derivative of (A5) at  $x = 0$  gives the relation

$$-\left(\frac{dc_1}{dx}\right)_{x=0} = \left(\frac{dc_2}{dx}\right)_{x=0} = \frac{c_0}{a} \quad (\text{A6})$$

See Figure 6 for the geometric meaning of the characteristic distance  $a$ . The second derivative of (A5) at  $x = 0$  gives the following relation

$$c_0 \left(\frac{d^2c_1}{dx^2}\right)_{x=0} + c_0 \left(\frac{d^2c_2}{dx^2}\right)_{x=0} + 2 \left(\frac{dc_1}{dx}\right)_{x=0} \left(\frac{dc_2}{dx}\right)_{x=0} = 0 \quad (\text{A7})$$

Based on (A3)-(A7)

$$\left(\frac{d^2c_1}{dx^2}\right)_{x=0} = \left(\frac{d^2c_2}{dx^2}\right)_{x=0} = \frac{c_0}{a^2} \quad (\text{A8})$$

and regarding (A3), (A4), and (A8), we obtain

$$D_{X^-}/a^2 = k_c c_0 \quad (\text{A9})$$

We need another equation to calculate  $a$  or  $c_0$ . (A9) was derived by using the reaction layer concept. Another relationship can be found by applying the diffusion layer concept as the reaction is fed by a diffusion current. As we have a symmetrical problem, half of the reaction takes place where  $x < 0$  and the other half in the region of  $x > 0$ . Consequently, the diffusion current density of component C entering into the diffusion layer of thickness  $\delta$

$$(J_c)_{x=\delta} = -D_c(dc_2/dx)_{x=\delta} \approx -D_c([C]_b/\delta) \quad (\text{A10})$$

will be halved at  $x = 0$

$$(J_c)_{x=0} = -D_c(dc_2/dx)_{x=0} = 1/2(J_c)_{x=\delta} \quad (\text{A11})$$

Regarding (A10), (A11) and (A6), we obtain

$$c_0/a = 1/2([C]_b/\delta) \quad (\text{A12})$$

where " $a$ " can be expressed from (A9) and (A12) as

$$a = \left(\frac{2\delta D_{X^-}}{[C]_b k_c}\right)^{1/3} \quad (\text{A13})$$

The last step of the present derivation is to show that most of the reaction takes place in the domain  $-a < x < +a$ . The reaction density  $R_c$  (the rate of the consumption of C per unit area of the electrode) between  $x = -a$  and  $x = +a$

$$R_c = \int_{-a}^{+a} r_c dx \quad (\text{A14})$$

where

$$r_c = \frac{k_c}{z} [X^-][C] \quad (\text{A15})$$

With (A2) and (A5)

$$r_c = \frac{D_c}{D_{X^-}} k_c c_1 c_2 = \frac{D_c}{D_{X^-}} k_c c_0^2 \quad (\text{A16})$$

and  $R_c$

$$R_c = \frac{D_c}{D_{X^-}} k_c c_0^2 (2a) \quad (\text{A17})$$

It can be shown by using (A12) and (A13) that

$$c_0^2 (2a) = \frac{D_{X^-} [C]_b}{k_c \delta} \quad (\text{A18})$$

and regarding (A17) and (A18), we obtain

$$R_c = D_c([C]_b/\delta) = |(J_c)_{x=\delta}| \quad (\text{A19})$$

That is, the whole current density of "C" entering into the diffusion layer is used up by the reaction in the region  $-a < x < +a$ . In other words, the above region is the reaction layer the thickness of which

$$\mu = 2a \quad (\text{A20})$$

and with (A12)

$$\mu \approx 2.5 \left(\frac{\delta D_{X^-}}{[C]_b k_c}\right)^{1/3} \quad (\text{A21})$$

**Registry No.** Br<sup>-</sup>, 24959-67-9; I<sup>-</sup>, 20461-54-5; HBrO<sub>2</sub>, 37691-27-3; HIO<sub>2</sub>, 30770-97-9; HBrO<sub>3</sub>, 7789-31-3; HIO<sub>3</sub>, 7782-68-5; H<sub>2</sub>SO<sub>4</sub>, 7664-93-9.

## Tricopper. A Fluxional Molecule

D. P. DiLella, K. V. Taylor, and M. Moskovits\*

Lash Miller Chemical Laboratories, Department of Chemistry, University of Toronto, Toronto, Ontario, Canada (Received: July 30, 1982)

The resonance Raman spectrum of matrix-isolated Cu<sub>3</sub> is reported. On the basis of the irregularity of the observed progression and the unusual isotopic structure shown by the vibrational spectral components, Cu<sub>3</sub> is proposed to be a fluxional Jahn-Teller molecule. A symmetric stretching frequency of 354 cm<sup>-1</sup> is found for the molecule.

The UV-visible absorption spectroscopy copper cluster species isolated in rare gas matrices has been the subject of numerous papers.<sup>1</sup> Although spectral features ascrib-

able to aggregates consisting of as many as four atoms have been reported, the lack of vibrational structure in these has made speculation into the geometries of these species difficult. In any case such conclusions, being drawn from absorption spectra, would have been pertinent only to the excited state.

Molecular orbital calculations on Cu<sub>x</sub> species have been

(1) H. Huber, E. P. Kündig, M. Moskovits, and G. A. Ozin, *J. Am. Chem. Soc.*, **97**, 2097 (1975); M. Moskovits and J. E. Hulse, *J. Chem. Phys.*, **67**, 4271 (1977).